Continuum defect mechanics and Fast Fourier transform (FFT) based numerical implementations with some applications

Stéphane Berbenni

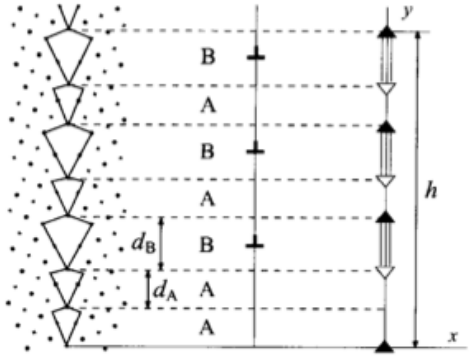
Laboratoire d'Etude des Microstructures et de Mécanique des Matériaux,
LEM3, UMR 7239, CNRS / LABEX 'DAMAS',
Université de Lorraine, F-57070 Metz, France

Acknowlegments: Komlan S. Djaka*, Julien Genée**, Xiaolei Chen***,
Vincent Taupin , Claude Fressengeas, Ricardo Lebensohn (LANL)
*former PhD (2014-2018) * *former post-doc (2018-2020),***former Post-doc (2021-2023)

GDR "Géometrie Différentielle et Mécanique »
(GDM) Différents points de vue sur la théorie des dislocations: physique, mécanique, mathématiques

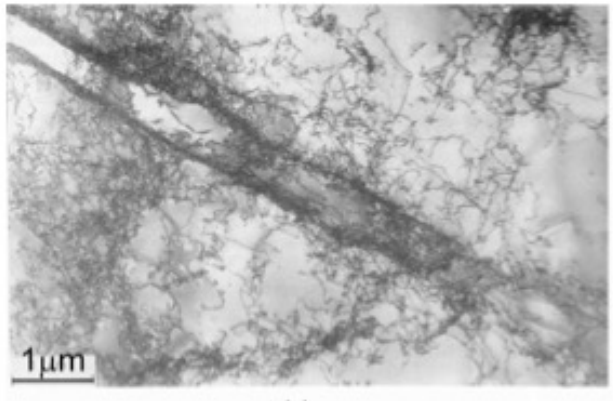
Defects in crystalline materials (dislocations, disclination –type defects) nano & micro scales

- Grain boundaries, GB defects, Nanocrystalline metals,...



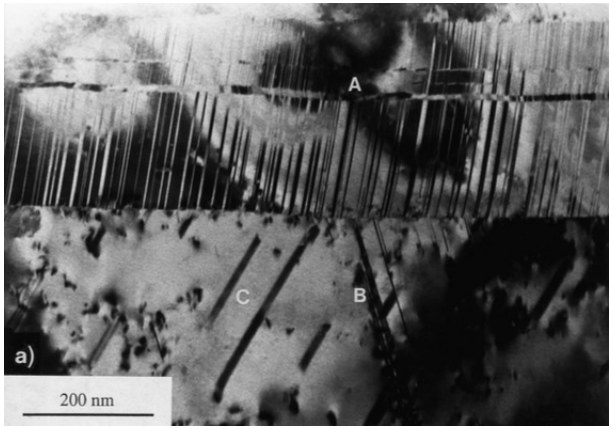
V. Yu. Gertsman et al. Philos. Mag. A 59 (1989)
A.A. Nazarov, A.E. Romanov, Philos. Mag. Lett. (1989)
M. Upadhyay et al. IJSS (2011),
C. Fressengeas et al. IJSS (2011,2014)

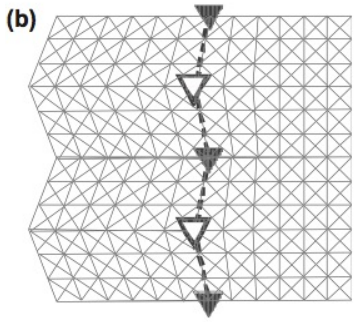
- Misorientation bands, micro bands,...



A.E. Romanov, A.L. Kolesnikova.
Prog. Mater. Sci (2009)

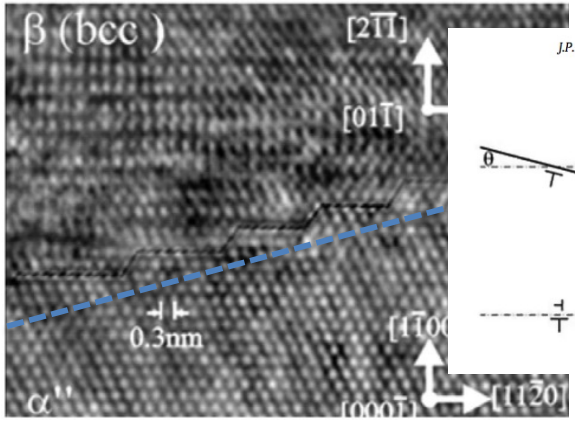
- Twin boundaries and twin junctions

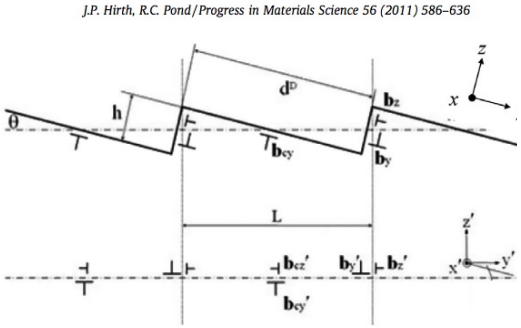




P. Müllner, A.H. King, Acta Mater (2010)

- GB terrace disconnection defects



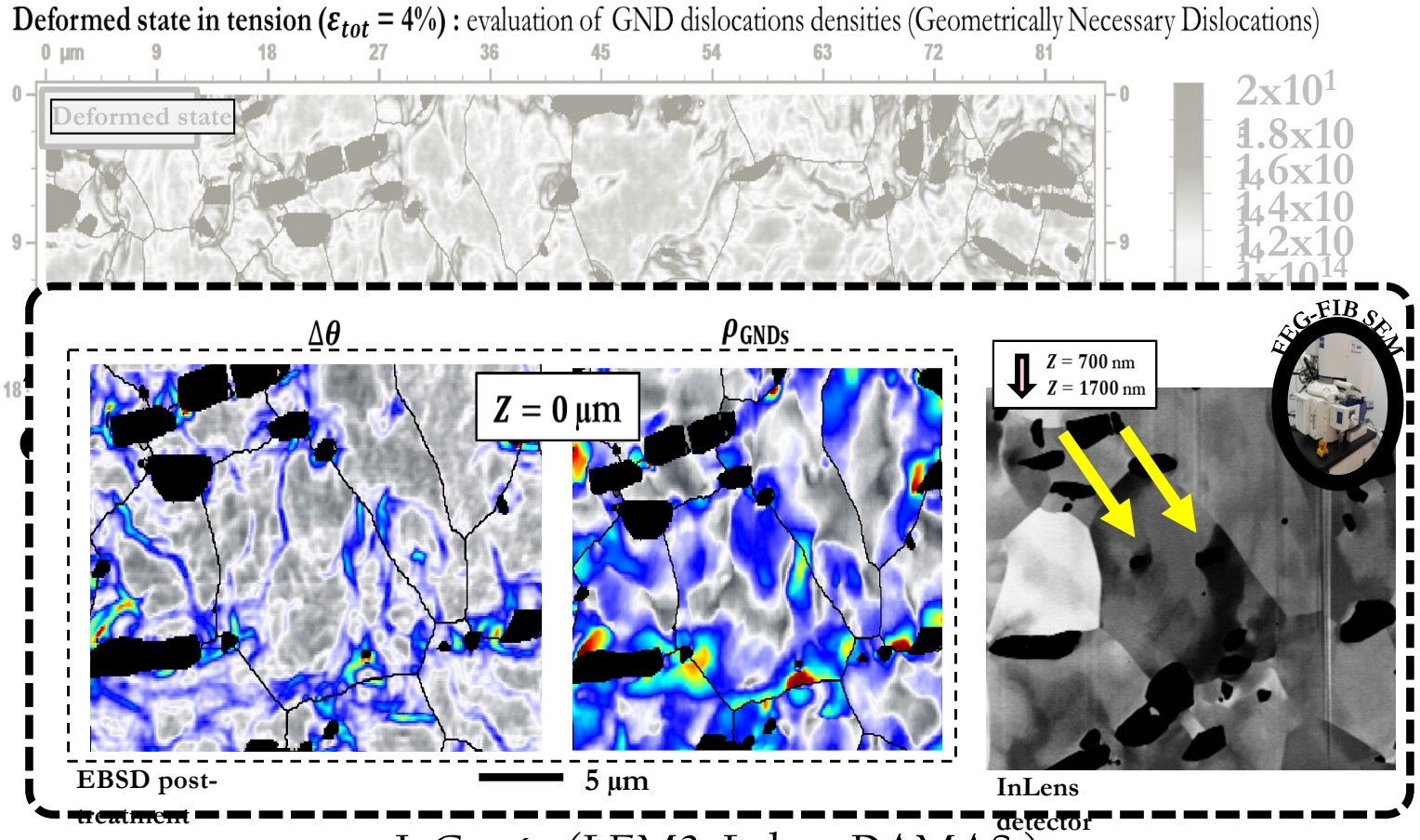


R.C. Pond et al. Acta Mater 51 (2003)
J.P. Hirth, R.C. Pond Prog. Mater 56 (2011)

Study of plastic deformation heterogeneities at mesoscale

Caracterization of deformed state

/ Localization of plastic deformation /



J. Genée (LEM3, Labex DAMAS)

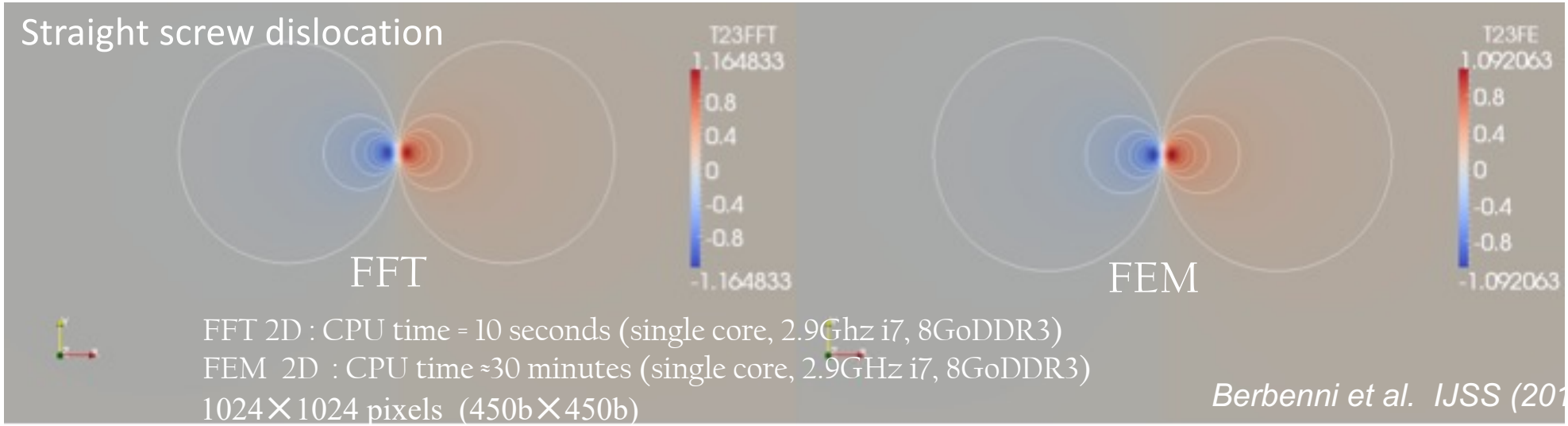
Motivations

Mesoscale Field Dislocation Mechanics (MFDM) for polycrystals?

Problem : implementation with 3D finite elements is CPU time consuming (*Acharya and Roy 2006, Puri et al. 2011, 2012, Richeton et al 2011, 2017, Arora-Acharya 2020:* bicrystals,multicrystals nanolayers, ...)

Need a fast method to compute mechanical fields : Fast Fourier Transform (FFT)

- **Composites:** *Moulinec-Suquet (1994, 1998)*, **Polycrystals** : *Lebensohn (2001)* **(VPFFT)**, Lebensohn et al. (2012) **(EVPFFT)** *then method developed by many groups, see review by : Lucarini1, Upadhyay, Segurado (2022), Schneider (2021)*
- **SG-EVPFFT** *(Lebensohn and Needleman, 2016)*, Large strain: **LS - SG-EVPFFT** *(Zecevic et al., 2023)*
- **FDM-FFT:** *Brenner et al. 2014, Berbenni et al. 2014, Djaka et al. 2015, 2017;* Disclin-FFT **(***Berbenni and Taupin, 2018)*
- **DDD-FFT**: *Bertin, Capolungo et al 2015; Graham et al. 2016;* **Eigenstrain-FFT** *(Anglin et al., 2014, Eloh et al., 2019)*
- Phase field -FFT *(Ruffini and Finel., 2015 ; Rodney et al., 2003 Chen et al , Koslowski, Hunter , Beyerlein et al. ...)*



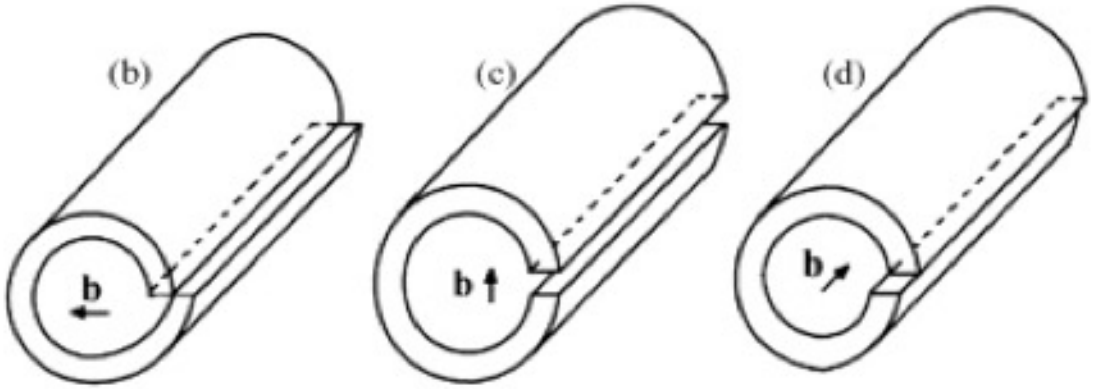
Talk: Stress fields of static defects and MFDM-EVPFFT model with applications

Outline

- Kinematics of dislocations and disclinations and Elasto-statics equations for heterogeneous media
- FFT-numerical resolution and some applications
- Mesoscopic Field Dislocation Mechanics (MFDM)
- Numerical implementation based on an elastoviscoplastic FFT scheme (MFDM-EVPFFT)
- Applications of MFDM-EVPFFT
- Summary and outlook

- Kinematics of dislocations and disclinations and Elasto-statics equations for heterogeneous media
- FFT-numerical resolution and some applications
- Mesoscopic Field Dislocation Mechanics (MFDM)
- Numerical implementation based on an elastoviscoplastic FFT scheme (MFDM-EVPFFT)
- Applications of MFDM-EVPFFT
- Summary and outlook

Kinematics of dislocations (small strains)



V. Volterra, Ann. Sci. Ec. Norm. Sup. III **24**, 401 (1907)

- Discontinuity of displacement along a Burgers circuit C (closed surface S): Burgers vector **b** (multi-valued displacement)

$$\left[\mathbf{u}\right] = \mathbf{b} = \int_C \mathbf{U}_e \mathbf{dx} = \int_S \mathbf{curl}\mathbf{U}_e \cdot \mathbf{n}\, \mathbf{dS} = \int_S \boldsymbol{\alpha} \cdot \mathbf{n}\, \mathbf{dS} \quad \begin{cases} \boldsymbol{\alpha} = \mathbf{curl}\mathbf{U}_e \\ \mathbf{div}\boldsymbol{\alpha} = 0 \end{cases}$$

E. Kröner (1958, 1981)

- Incompatibility of elastic distortion $\mathbf{U}_e$

$\boldsymbol{\alpha}$: Nye tensor (dislocation density, Nye 1953)

- Stokes-Helmholtz decomposition (Kröner 1958, Acharya, 2001)

$$\mathbf{U}_e = \mathbf{U}_e^{\perp} + \mathbf{U}_e^{//} = \mathbf{curl}\ \boldsymbol{\chi} + \mathbf{grad}\ \mathbf{w} \quad \text{with} \quad \begin{cases} \mathbf{div}\ \mathbf{U}_e^{\perp} = \mathbf{0} \\ \mathbf{curl}\ \mathbf{U}_e^{//} = \mathbf{0} \end{cases}$$

- Poisson equation (Berbenni et al. IJSS 2014):

$$\boldsymbol{\alpha} = \mathbf{curl}\ \mathbf{U}_e^{\perp} \Rightarrow \mathbf{div}\ \mathbf{grad}\ \mathbf{U}_e^{\perp} = \Delta \mathbf{U}_e^{\perp} = -\mathbf{curl}\ \boldsymbol{\alpha}$$

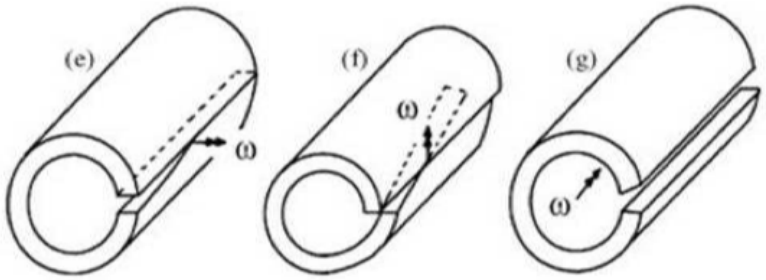
Kinematics of disclinations (small strains)

- Discontinuity of rotation along a closed circuit C (and surface S inside it): Frank's vector $\boldsymbol{\Omega}$

$$\left[\vec{\omega}\right] = \boldsymbol{\Omega} = \int_C \boldsymbol{\kappa}_e \cdot \mathbf{dx} = \int_S \mathbf{curl}\boldsymbol{\kappa}_e \cdot \mathbf{n}\, \mathbf{dS} = \int_S \boldsymbol{\theta} \cdot \mathbf{n}\, \mathbf{dS}$$

$$\mathbf{b} = \int_C \left(\boldsymbol{\varepsilon}_e - \boldsymbol{\kappa}_e \times \mathbf{x}\right) \cdot \mathbf{dx} = \int_S \left(\boldsymbol{\alpha} - \boldsymbol{\theta} \times \mathbf{x}\right) \cdot \mathbf{n}\, \mathbf{dS}$$

R. DeWit (1970)



V. Volterra, Ann. Sci. Ec. Norm. Sup. III **24**, 401 (1907)

- Incompatibility of elastic curvature $\boldsymbol{\kappa}_e$: $\boldsymbol{\theta} = \mathbf{curl}\boldsymbol{\kappa}_e$ with $\mathbf{div}\boldsymbol{\alpha} + 2\vec{\boldsymbol{\theta}} = 0$ with $\vec{\boldsymbol{\theta}} = -\frac{1}{2}\boldsymbol{\theta} : \mathbf{X}$
- Incompatibility of elastic strain $\boldsymbol{\varepsilon}_e$: $\mathbf{curl}\,\boldsymbol{\varepsilon}_e + tr(\boldsymbol{\kappa}_e)\mathbf{I} - \boldsymbol{\kappa}_e^t = \boldsymbol{\alpha}$
- Elastic rotation tensor is multi-valued (undefined)
- Stokes-Helmholtz decomposition: $\boldsymbol{\kappa}_e = \boldsymbol{\kappa}_e^{\perp} + \boldsymbol{\kappa}_e^{//}$; $\boldsymbol{\varepsilon}_e = \boldsymbol{\varepsilon}_e^{\perp} + \boldsymbol{\varepsilon}_e^{//}$

- Two successive Poisson equations:

$$\boldsymbol{\theta} = \mathbf{curl}\ \boldsymbol{\kappa}_e^{\perp} \Rightarrow \mathbf{div\ grad}\ \boldsymbol{\kappa}_e^{\perp} = \Delta\boldsymbol{\kappa}_e^{\perp} = -\mathbf{curl}\ \boldsymbol{\theta}$$

$$\Delta\boldsymbol{\varepsilon}_e^{\perp} = -\mathbf{curl}\left(\boldsymbol{\alpha} - tr\left(\boldsymbol{\kappa}_e^{\perp}\right)\mathbf{I} + \boldsymbol{\kappa}_e^{t\perp}\right)$$

Elasto-static fields equations for defects in heterogeneous materials

Field Dislocation Mechanics

- Stokes-Helmholtz decomposition

$$\mathbf{U}_e = \mathbf{U}_e^{\perp} + \mathbf{U}_e^{\parallel} = \mathbf{curl}\,\boldsymbol{\chi} + \mathbf{grad}\,\mathbf{w}$$

- Poisson-type equation for incompatible elastic fields

$$\Delta \mathbf{U}_e^{\perp} = -\mathbf{curl}\,\boldsymbol{\alpha} \qquad (1)$$

Field Disclination Mechanics

$$\boldsymbol{\kappa}_e = \boldsymbol{\kappa}_e^{\perp} + \boldsymbol{\kappa}_e^{//} \quad \text{and}$$

$$\boldsymbol{\varepsilon}_e = \boldsymbol{\varepsilon}_e^{\perp} + \boldsymbol{\varepsilon}_e^{//}$$

$$\Delta \boldsymbol{\kappa}_e^{\perp} = -\mathbf{curl}\;\boldsymbol{\theta}$$

$$\Delta \boldsymbol{\varepsilon}_e^{\perp} = -\mathbf{curl}\;\left(\boldsymbol{\alpha} - tr\left(\boldsymbol{\kappa}_e^{\perp}\right)\mathbf{I} + \boldsymbol{\kappa}_e^{\perp t}\right) \qquad (1)$$

- Lippmann-Schwinger integral equation for compatible elastic strain

$$(2)\quad \varepsilon_{ij}^{e,\parallel}(\mathbf{x}) = \left\langle \varepsilon^{e,\parallel} \right\rangle_{ij} - \int_V \Gamma^0_{ijkl}(\mathbf{x}-\mathbf{x}')\tau_{kl}(\mathbf{x}')\,dV'$$

with

$$\tau_{ij} = T_{ij}^{\perp} + \delta C_{ijkl}\varepsilon_{kl}^{e,\parallel}$$

$$T_{ij}^{\perp} = C_{ijkl}\varepsilon_{kl}^{e,\perp}$$

- Kinematics of dislocations and disclinations and Elasto-statics equations for heterogeneous media
- **FFT-numerical resolution and some applications**
- Mesoscopic Field Dislocation Mechanics (MFDM)
- Numerical implementation based on an elastoviscoplastic FFT scheme (MFDM-EVPFFT)
- Applications of MFDM-EVPFFT
- Summary and outlook

Spectral approach of elasto-static field equations

- Incompatible fields:

Field Dislocation Mechanics

1

$$\begin{cases} \tilde{U}_{ij}^{e,\perp}(\xi) = \dfrac{i}{\xi^2}\xi_k\left(e_{jkl}\tilde{\alpha}_{il}(\xi)\right) & \forall \xi \neq \mathbf{0} \\ \tilde{U}_{ij}^{e,\perp}(\mathbf{0}) = \mathbf{0} \end{cases}$$

(Berbenni et al. IJSS 2014)

Field Disclination Mechanics

$$\begin{cases} \tilde{\kappa}_{ij}^{e,\perp}(\xi) = \dfrac{i}{\xi^2}\xi_k\left(e_{jkl}\tilde{\theta}_{il}(\xi)\right) & \forall \xi \neq \mathbf{0} \\ \tilde{\kappa}_{ij}^{e,\perp}(\mathbf{0}) = \mathbf{0} \end{cases}$$

$$\begin{cases} \tilde{\varepsilon}_{ij}^{e,\perp}(\xi) = \dfrac{i}{\xi^2}\xi_k e_{jkl}\left(\tilde{\alpha}_{il}(\xi) + \tilde{\kappa}_{li}^{e,\perp}(\xi) - \delta_{il}\tilde{\kappa}_{pp}^{e,\perp}(\xi)\right) & \forall \xi \neq \mathbf{0} \\ \tilde{\varepsilon}_{ij}^{e,\perp}(\mathbf{0}) = \mathbf{0} \end{cases}$$

(Berbenni et al, this work)

- Lippmann-Schwinger-type equation with incompatibilities:

2

$$\varepsilon_{ij}^{e,\|}(\mathbf{x}) = \left\langle \varepsilon^{e,\|} \right\rangle_{ij} - \int_V \Gamma_{ijkl}^0(\mathbf{x}-\mathbf{x}')\tau_{kl}(\mathbf{x}')dV' \Rightarrow$$

$$\begin{cases} \tilde{\varepsilon}^{e,\|}(\xi) = -\tilde{\Gamma}^0(\xi) : \tau(\xi) & \forall \xi \neq \mathbf{0} \\ \tilde{\varepsilon}^{e,\|}(\mathbf{0}) = \left\langle \varepsilon^{e,\|} \right\rangle \end{cases}$$

(Djaka et al., CMAME 2017)

$$\tilde{\Gamma}_{ijkl}^0(\xi) = \frac{1}{4}\left(\tilde{G}_{ik}^0(\xi)\xi_l\xi_j + \tilde{G}_{jk}^0(\xi)\xi_l\xi_i + \tilde{G}_{il}^0(\xi)\xi_k\xi_j + \tilde{G}_{jl}^0(\xi)\xi_k\xi_i\right)$$

$$\begin{cases} \tilde{G}_{ik}^0(\xi) = \left(\xi_j C_{ijkl}^0 \xi_l\right)^{-1} & \forall \xi \neq \mathbf{0} \\ \tilde{G}_{ik}^0(\mathbf{0}) = \mathbf{0} \end{cases}$$

(Mura 1987)

- Different iterative schemes to solve Lippmann-Schwinger equation
  - Basic Scheme (Moulinec-Suquet 1994,1998)
  - Accelerated Scheme (Eyre-Milton 1999)
  - Augmented Lagrangian (Michel et al. 2001)
  - Conjugate Gradient (Zeman et al, 2010, ...)

Convergence is dependent on the choice of the reference medium C^0 (see Michel et al. 2001)

FFT-based algorithm (Dislocation defects)

Initialization ($\boldsymbol{\alpha}$ being known)

1: $\tilde{\alpha} \leftarrow \mathrm{FFT}(\alpha)$

2: Solve Poisson's equation to obtain $\tilde{\mathbf{U}}^{e,\perp}$

$$\begin{cases} \tilde{U}_{ij}^{e,\perp}(\xi) = \dfrac{i}{\xi^2}\xi_k\left(e_{jkl}\tilde{\alpha}_{il}(\xi)\right) & \forall \xi \neq \mathbf{0} \\ \tilde{U}_{ij}^{e,\perp}(\mathbf{0}) = \mathbf{0} \end{cases}$$

3: $\mathbf{U}^{e,\perp} \leftarrow \mathrm{FFT}^{-1}(\tilde{\mathbf{U}}^{e,\perp})$

4: $\mathbf{T}^{\perp} \leftarrow \mathbf{C} : \boldsymbol{\varepsilon}^{e,\perp}$

5: $\boldsymbol{\varepsilon}_0^{e,\parallel} \leftarrow \langle \boldsymbol{\varepsilon}^{e,\parallel} \rangle = \mathbf{C}^{0^{-1}} : \bar{\mathbf{T}}$

6: $\mathbf{T}_0 \leftarrow \mathbf{C} : \boldsymbol{\varepsilon}_0^{e,\parallel} + \mathbf{T}^{\perp}$

Djaka et al. (CMAME 2017)

Iteration n+1: ($\mathbf{T_n}$ and $\boldsymbol{\varepsilon}_n^{e,\parallel}$ being known)

7: $\tilde{\mathbf{T}}_n = \mathrm{FFT}(\mathbf{T}_n)$

8: Convergence test (sress equilibrium):

$$e_n = \frac{\left(\frac{1}{N}\sum_{i=1}^{N} |\boldsymbol{\xi}_i . \hat{\boldsymbol{\sigma}}_n(\boldsymbol{\xi}_i)|^2\right)^{1/2}}{\|\hat{\boldsymbol{\sigma}}_n(\mathbf{0})\|_F} \leq \epsilon$$

9: $\tilde{\boldsymbol{\tau}}_n(\xi) \leftarrow \tilde{\mathbf{T}}_n(\xi) - \widetilde{\left(\mathbf{C}^0 : \boldsymbol{\varepsilon}_n^{e,\parallel}(\xi)\right)}$

10: $\tilde{\boldsymbol{\varepsilon}}_{n+1}^{e,\parallel}(\xi) \leftarrow -\tilde{\Gamma}^0(\xi) : \tilde{\boldsymbol{\tau}}_n(\xi) \quad \forall \xi \neq \mathbf{0}$

$\tilde{\boldsymbol{\varepsilon}}_{n+1}^{e,\parallel}(\mathbf{0}) \leftarrow \langle \boldsymbol{\varepsilon}^{e,\parallel} \rangle$

11: $\boldsymbol{\varepsilon}_{n+1}^{e,\parallel} \leftarrow \mathrm{FFT}^{-1}(\tilde{\boldsymbol{\varepsilon}}_{n+1}^{e,\parallel}(\xi))$

12: $\mathbf{T}_{n+1} \leftarrow \mathbf{C} : \boldsymbol{\varepsilon}_{n+1}^{e,\parallel} + \mathbf{T}^{\perp}$

FFT-based algorithm (Disclination defects)

Initialization (θ, α being known)

1: $\tilde{\theta} \leftarrow \mathrm{FFT}(\theta)$

2: Solve 1st Poisson's equation to obtain $\tilde{\kappa}^{e,\perp}$

$$\begin{cases} \tilde{\kappa}^{e,\perp}_{ij}(\xi) = \dfrac{i}{\xi^2}\xi_k\left(e_{jkl}\tilde{\theta}_{il}(\xi)\right) & \forall \xi \neq \mathbf{0} \\ \tilde{\kappa}^{e,\perp}_{ij}(\mathbf{0}) = \mathbf{0} \end{cases}$$

3: Solve 2nd Poisson's equation to obtain $\tilde{\varepsilon}^{e,\perp}$

$$\begin{cases} \tilde{\varepsilon}^{e,\perp}_{ij}(\xi) = \dfrac{i}{\xi^2}\xi_k e_{jkl}\left(\tilde{\alpha}_{il}(\xi) + \tilde{\kappa}^{e,\perp}_{li}(\xi) - \delta_{il}\tilde{\kappa}^{e,\perp}_{pp}(\xi)\right) \\ \forall \xi \neq \mathbf{0} \qquad\qquad \tilde{\varepsilon}^{e,\perp}_{ij}(\mathbf{0}) = \mathbf{0} \end{cases}$$

4: $\boldsymbol{\varepsilon}^{e,\perp} \leftarrow \mathrm{FFT}^{-1}(\tilde{\boldsymbol{\varepsilon}}^{e,\perp})$

5: $\mathbf{T}^{\perp} \leftarrow \mathbf{C} : \boldsymbol{\varepsilon}^{e,\perp}$

6: $\boldsymbol{\varepsilon}^{e,\parallel}_0 \leftarrow \langle \boldsymbol{\varepsilon}^{e,\parallel} \rangle = \mathbf{C}^{0^{-1}} : \bar{\mathbf{T}}$

7: $\mathbf{T}_0 \leftarrow \mathbf{C} : \boldsymbol{\varepsilon}^{e,\parallel}_0 + \mathbf{T}^{\perp}$

Iteration n+1: ($\mathbf{T}_n$ and $\boldsymbol{\varepsilon}^{e,\parallel}_n$ being known)

8: $\tilde{\mathbf{T}}_n = \mathrm{FFT}(\mathbf{T}_n)$

9: Convergence test (stress equilibrium):

$$e_n = \frac{\left(\frac{1}{N}\sum_{i=1}^{N} |\boldsymbol{\xi}_i . \hat{\boldsymbol{\sigma}}_n(\boldsymbol{\xi}_i)|^2\right)^{1/2}}{\|\hat{\boldsymbol{\sigma}}_n(\mathbf{0})\|_F} \leq \epsilon$$

10: $\tilde{\boldsymbol{\tau}}_n(\xi) \leftarrow \tilde{\mathbf{T}}_n(\xi) - \widetilde{\left(\mathbf{C}^0 : \boldsymbol{\varepsilon}^{e,\parallel}_n(\xi)\right)}$

11: $\tilde{\boldsymbol{\varepsilon}}^{e,\parallel}_{n+1}(\xi) \leftarrow -\tilde{\Gamma}^0(\xi) : \tilde{\boldsymbol{\tau}}_n(\xi) \qquad \forall \xi \neq \mathbf{0}$

$\tilde{\boldsymbol{\varepsilon}}^{e,\parallel}_{n+1}(\mathbf{0}) \leftarrow \langle \boldsymbol{\varepsilon}^{e,\parallel} \rangle$

12: $\boldsymbol{\varepsilon}^{e,\parallel}_{n+1} \leftarrow \mathrm{FFT}^{-1}(\tilde{\boldsymbol{\varepsilon}}^{e,\parallel}_{n+1}(\xi))$

13: $\mathbf{T}_{n+1} \leftarrow \mathbf{C} : \boldsymbol{\varepsilon}^{e,\parallel}_{n+1} + \mathbf{T}^{\perp}$

Approximations for differentiation rules in the Fourier space (from Discrete Fourier Transform)

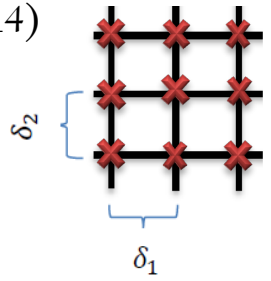
- Classic approximation (Moulinec et Suquet 1994, 1998) $\dfrac{\partial}{\partial x_j} \Leftrightarrow i\xi_j = \dfrac{i2\pi}{T_j} m_j$

- Poisson : P_C → Centered finite difference (stencil) approximation (Berbenni IJSS 2014)

$$\frac{\partial^2 f(i,j)}{\partial x_1^2} = \frac{f(i+1,j) - 2f(i,j) + f(i-1,j)}{\delta_1^2}$$
$$\frac{\partial^2 f(i,j)}{\partial x_2^2} = \frac{f(i,j+1) - 2f(i,j) + f(i,j-1)}{\delta_2^2}$$
$$\frac{\partial^2 f(i,j)}{\partial x_1 \partial x_2} = \frac{f(i+1,j+1) - f(i+1,j-1) - f(i-1,j+1) + f(i-1,j-1)}{4\delta_1\delta_2}$$

$\Leftrightarrow$

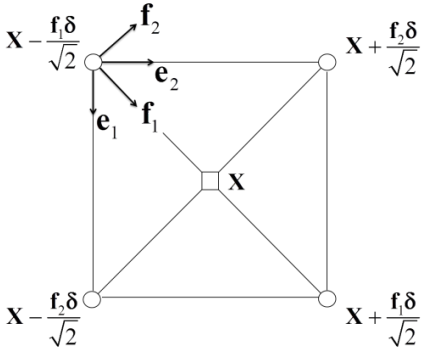
$$-\xi_1^2 \leftrightarrow \frac{2}{\delta_1^2}\left(\cos\left(\frac{2\pi(k-1)}{N_1}\right) - 1\right)$$
$$-\xi_2^2 \leftrightarrow \frac{2}{\delta_2^2}\left(\cos\left(\frac{2\pi(l-1)}{N_2}\right) - 1\right)$$



$$-\xi_1\xi_2 \leftrightarrow \frac{1}{2\delta_1\delta_2}\left[\cos\left(2\pi\left(\frac{(k-1)}{N_1} + \frac{(l-1)}{N_2}\right)\right) - \cos\left(2\pi\left(\frac{(k-1)}{N_1} - \frac{(l-1)}{N_2}\right)\right)\right]$$

- Lippmann-Schwinger : LS_R → Rotated centered difference scheme (Willot., 2015)

$$\frac{\partial}{\partial x_j} \Leftrightarrow i\xi_j^R = \frac{i}{4\delta}\tan\left(\frac{\pi m_j}{N_j}\right) \times \left(1 + \exp\left(i\frac{2\pi m_1}{N_1}\right)\right) \times \left(1 + \exp\left(i\frac{2\pi m_2}{N_2}\right)\right) \times \left(1 + \exp\left(i\frac{2\pi m_3}{N_3}\right)\right)$$



- Mixed- Procedure : P_C-LS_R (Djaka et al., CMAME 2017)

A simple example for static single dislocation problem

Real space

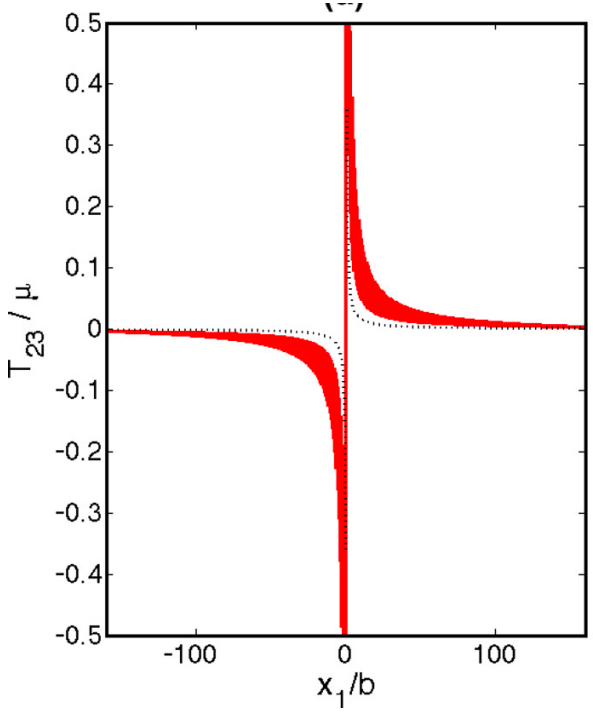
$$\mathbf{U_e = U_e^{\perp} + U_e^{//} = curl\ \chi + grad\ w} \quad \text{with} \begin{cases} \mathbf{div\ U_e^{\perp} = 0} \\ \mathbf{curl\ U_e^{//} = 0} \end{cases} \Longrightarrow$$

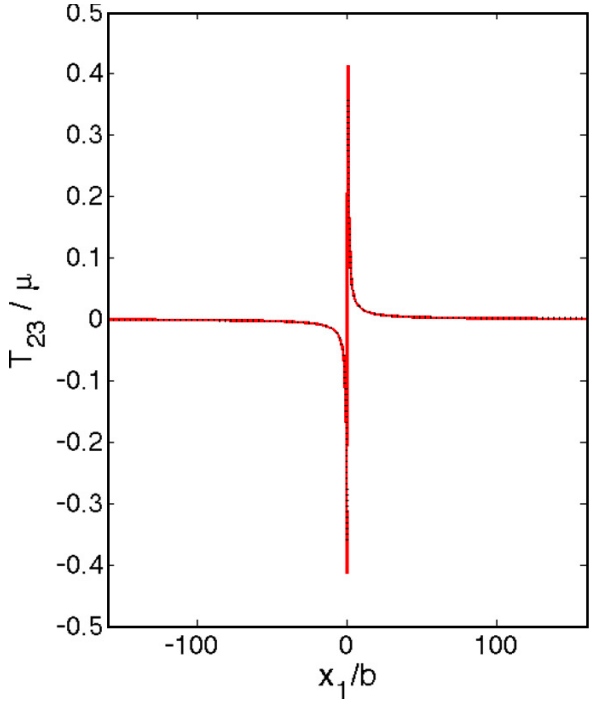
Fourier space (FFT)

$$\begin{cases} \tilde{U}_{ij}^{e,\perp}(\xi) = \dfrac{i}{\xi^2}\xi_k\left(e_{jkl}\tilde{\alpha}_{il}(\xi)\right) \ \forall \xi \neq 0 \\ \tilde{U}_{ij}^{e,\perp}(0) = 0 \end{cases}$$

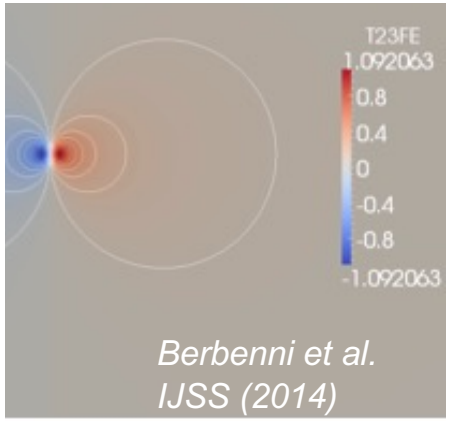
$$\mathbf{\alpha = curl\ U_e^{\perp} \Rightarrow div\ grad\ U_e^{\perp} = \Delta U_e^{\perp} = -curl\ \alpha}$$

$$\varepsilon_{ij}^{e,\|}(\mathbf{x}) = \langle \varepsilon^{e,\|} \rangle_{ij} - \int_V \Gamma^0_{ijkl}(\mathbf{x}-\mathbf{x}')\tau_{kl}(\mathbf{x}')dV' \quad \text{with} \begin{cases} \tau_{ij} = T_{ij}^{\perp} + \delta C_{ijkl}\varepsilon_{kl}^{e,\|} \\ T_{ij}^{\perp} = C_{ijkl}\varepsilon_{kl}^{e,\perp} \end{cases} \Longrightarrow \begin{cases} \tilde{\varepsilon}^{e,\|}(\xi) = -\tilde{\Gamma}^0(\xi) : \tau(\xi) \quad \forall \xi \neq 0 \\ \tilde{\varepsilon}^{e,\|}(0) = \langle \varepsilon^{e,\|} \rangle \end{cases}$$

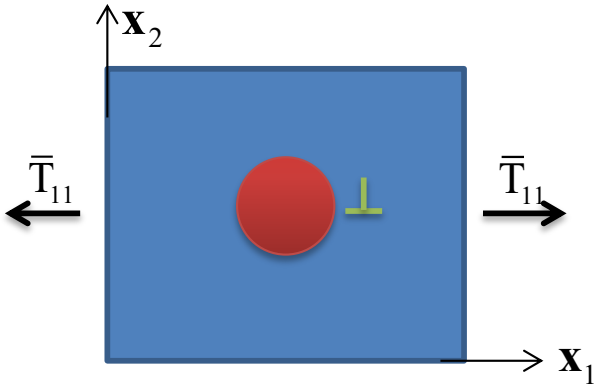




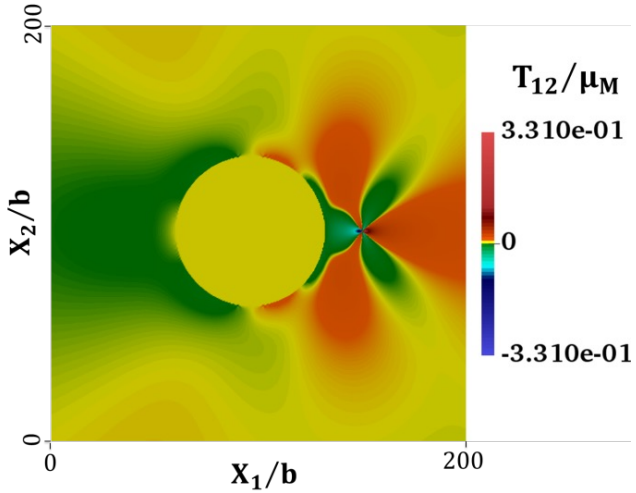
$_{33} = b/\delta^2$

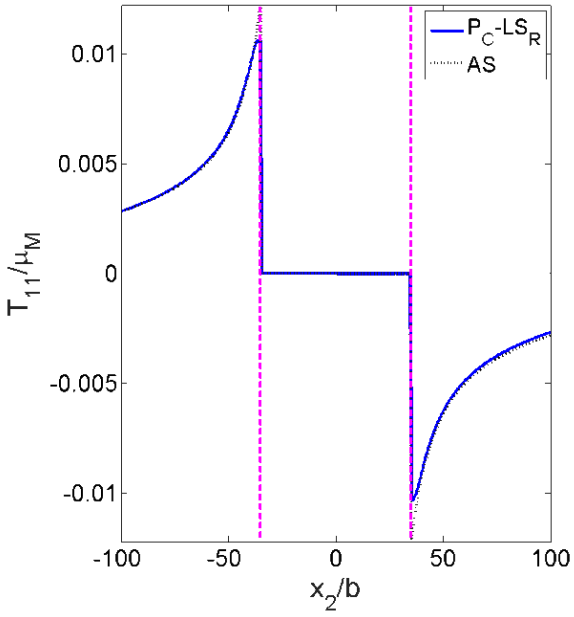


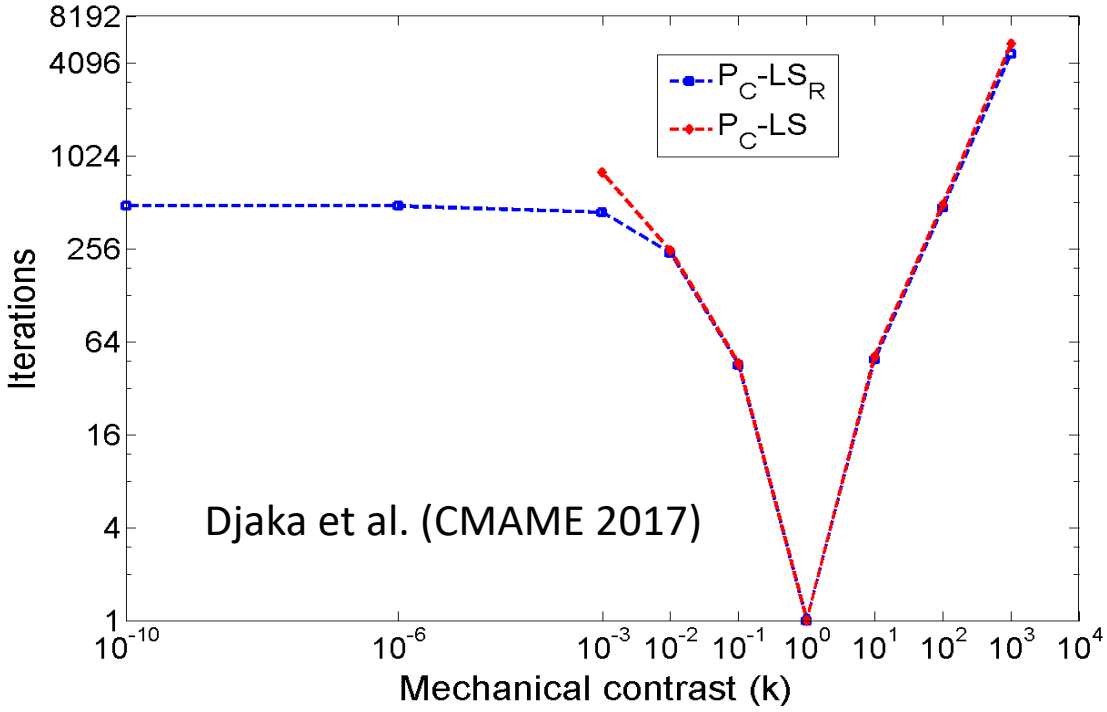
Interactions of dislocation with a hole with P_C-LS_R approximation for different contrasts



Elastic fields induced by an edge dislocation nearby a hole







$\varepsilon = 10^{-6}$

$\mu_M = 2.3001 \times 10^3 \text{MPa}; \nu_M = \nu_I = 0.3647$

$\mu_0 = 0.505(\mu_M + \mu_I)$

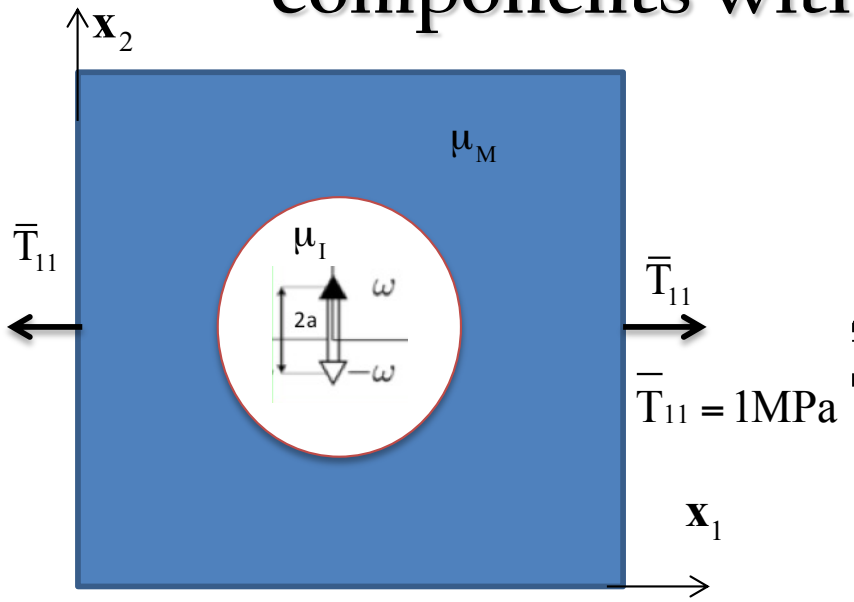
$\bar{T}_{11} = 1\text{MPa}$

- Analytical solutions

  Dundurs et Mura, 1964

➔ Convergence obtained for void interacting with dislocation with $\mathbf{P_C\text{-}LS_R}$

Application to wedge disclination dipoles: Stress components with a circular inhomogeneity



Rotation discontinuity (wedge disclination dipole, Frank pseudo-vector: $\pm\omega = \pm 5/6 rad$)

Disclination densities (on 1 pixel) (dipole at x2=±a): $\theta_{33}(\mathbf{x}) = \pm\omega/\delta^2$

Mesh: 1024×1024 pixels

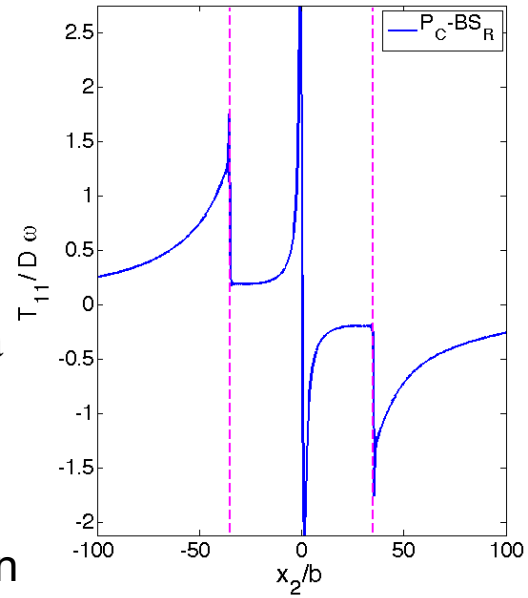
Pixel size: $\delta_1 = \delta_2 = \delta \simeq 0.44b$

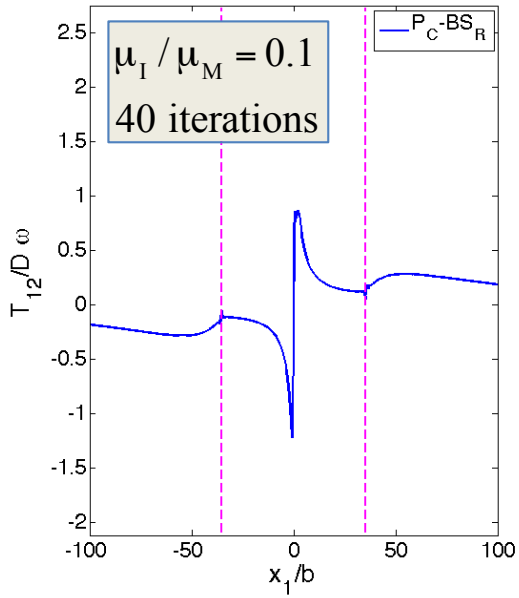
Inclusion radius: $R = 80\delta$

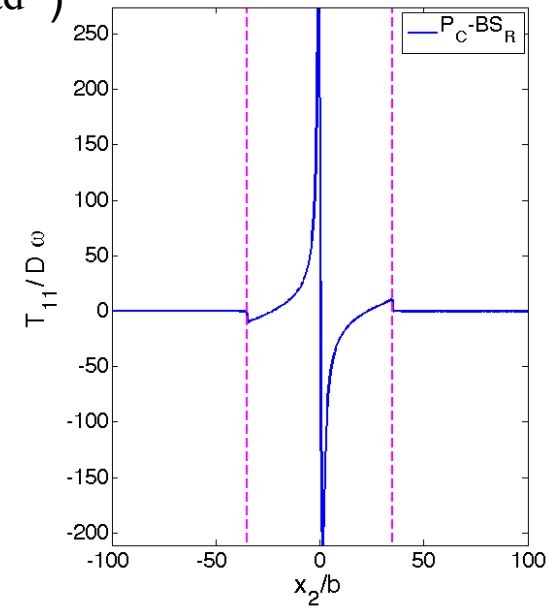
$\mu_M = 2.3001 \times 10^3 MPa;\ \nu_M = \nu_I = 0.3647$

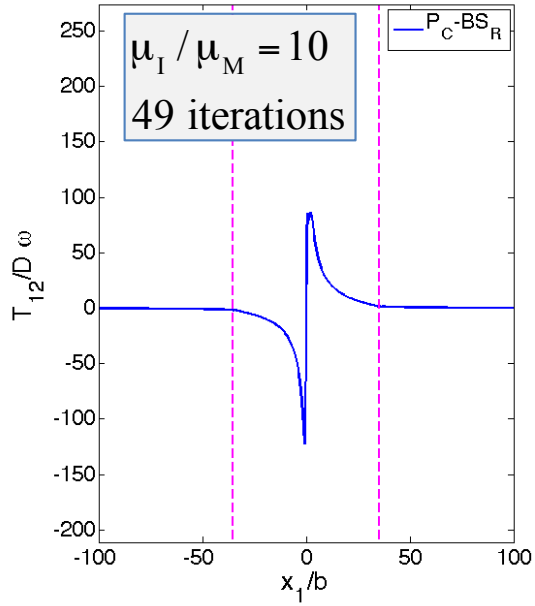
$\mu_0 = 0.505(\mu_M + \mu_I);\ D = \dfrac{\mu_M}{2\pi(1-\nu_M)}$

Convergence criteria: $\varepsilon = 10^{-6}$

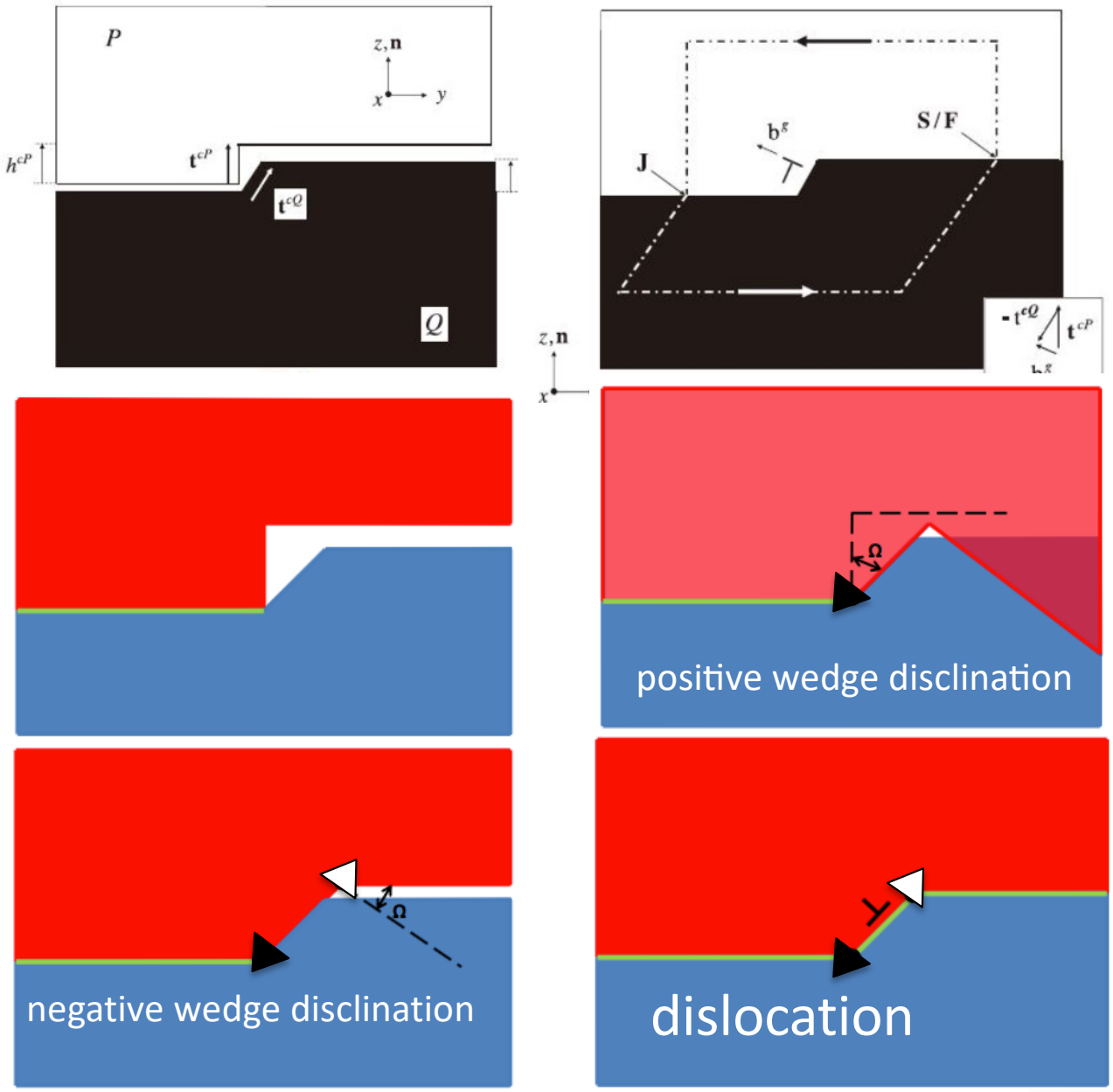








Applications to dislocation/disclination defects: Pond and Hirth's disconnection



Burgers circuit to define the equivalent Burgers vector of the disconnection *Hirth-Pond, Prog. Mater. Sci. (2011)*

Continuum defect mechanics description of the disconnection defect

1 disclination dipole

+ 1 dislocation

Pixel size: $\delta_1 = \delta_2 = \delta \simeq 0.44b$

$$\theta_{33}(\mathbf{x}) = \pm\omega/\delta^2 \quad \text{with } \omega = \pi/4$$

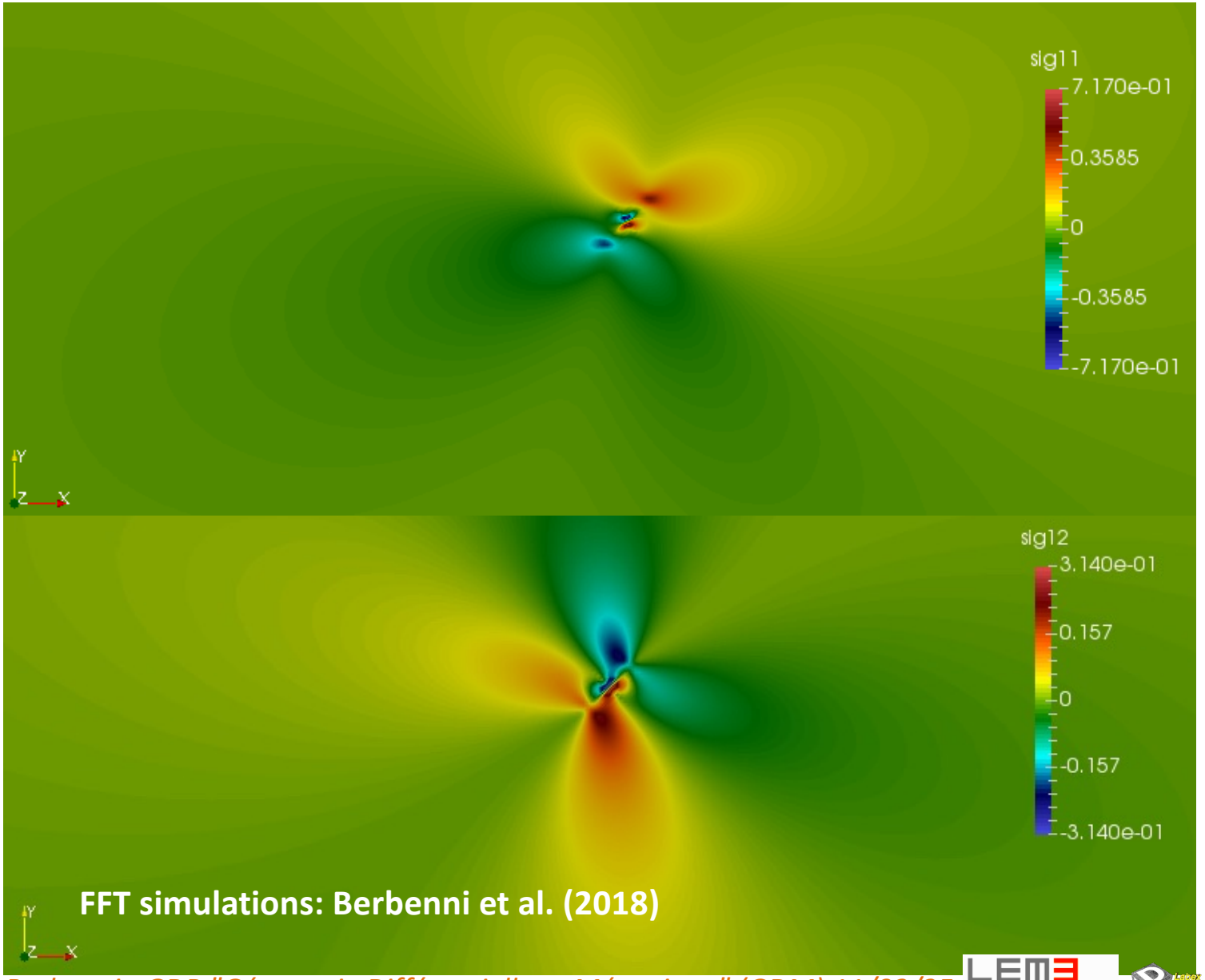
$$a = a_{Cu} = 0.3615\text{nm}$$

$$\alpha_{13}(\mathbf{x}) = a\cdot\cos\left(\frac{\pi}{4}\right)/\delta^2$$

$$\alpha_{23}(\mathbf{x}) = a\cdot\sin\left(\frac{\pi}{4}\right)/\delta^2$$

Predicted stress field

Mesh: 512×512 pixels

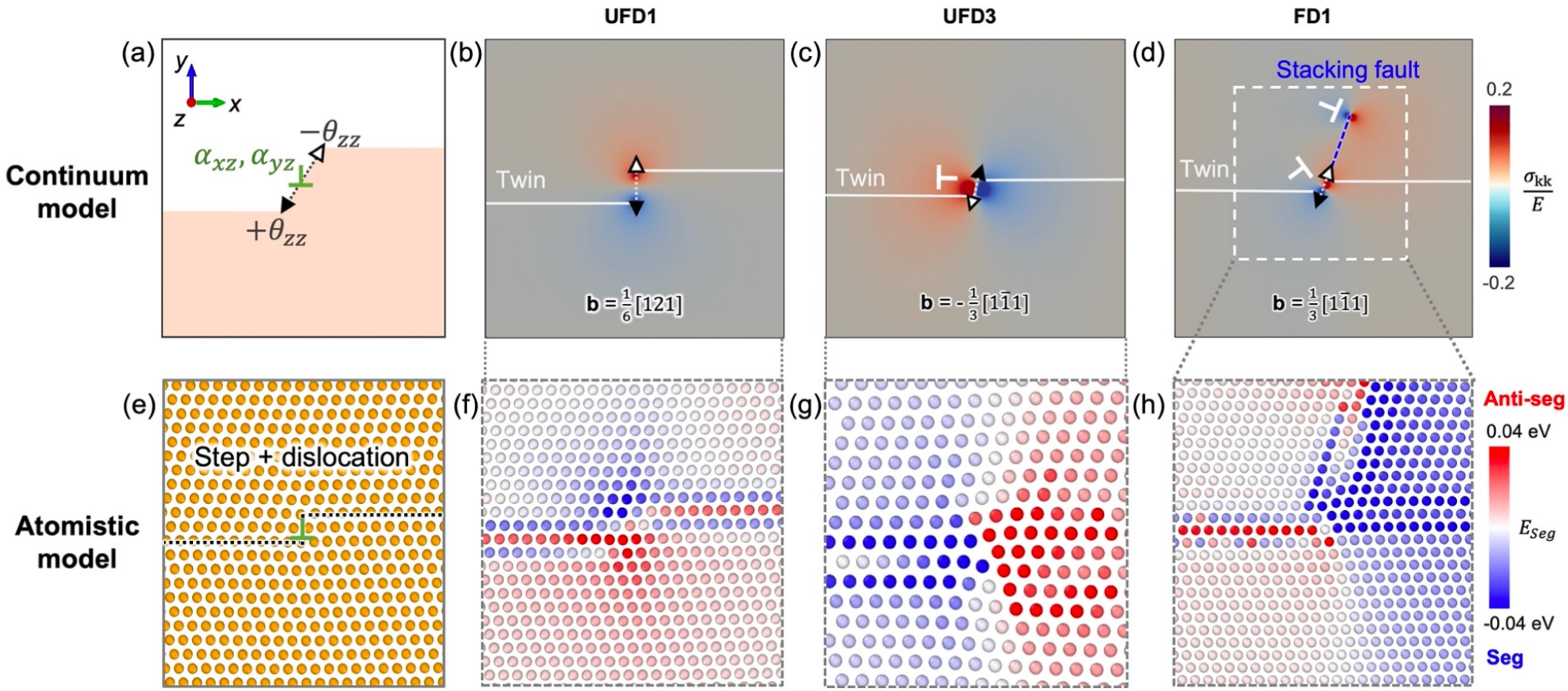


Isotropic elastic constants for Copper:

E_{Cu}=130GPa

ν_{Cu}=0.34

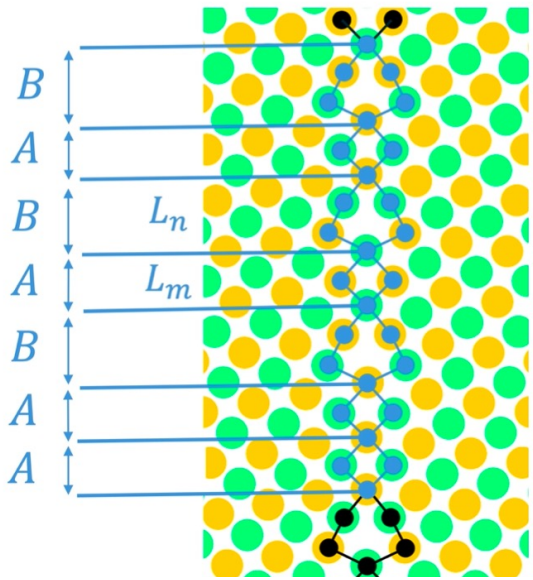
Comparison of normalized hydrostatic pressure distribution (continuum model) vs. segregation maps (MD) for three representative disconnections



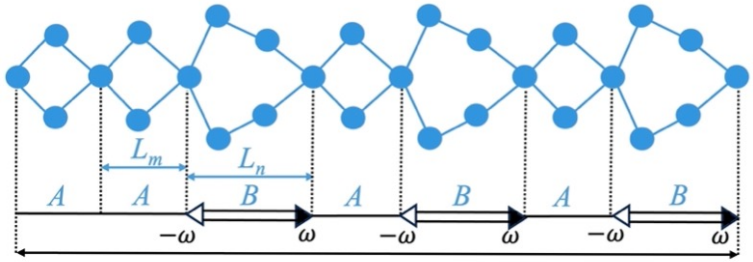
Hu, Berbenni, Medlin, Dingreville. Acta Mater. 246 (2023)

$$E_{\text{seg}} = E_{\text{twin}}^{\text{solute}} - E_{\text{bulk}}^{\text{solute}}$$

Application to HAGBs (High Angle Grain Boundaries): based on Disclination Structural Unit Model



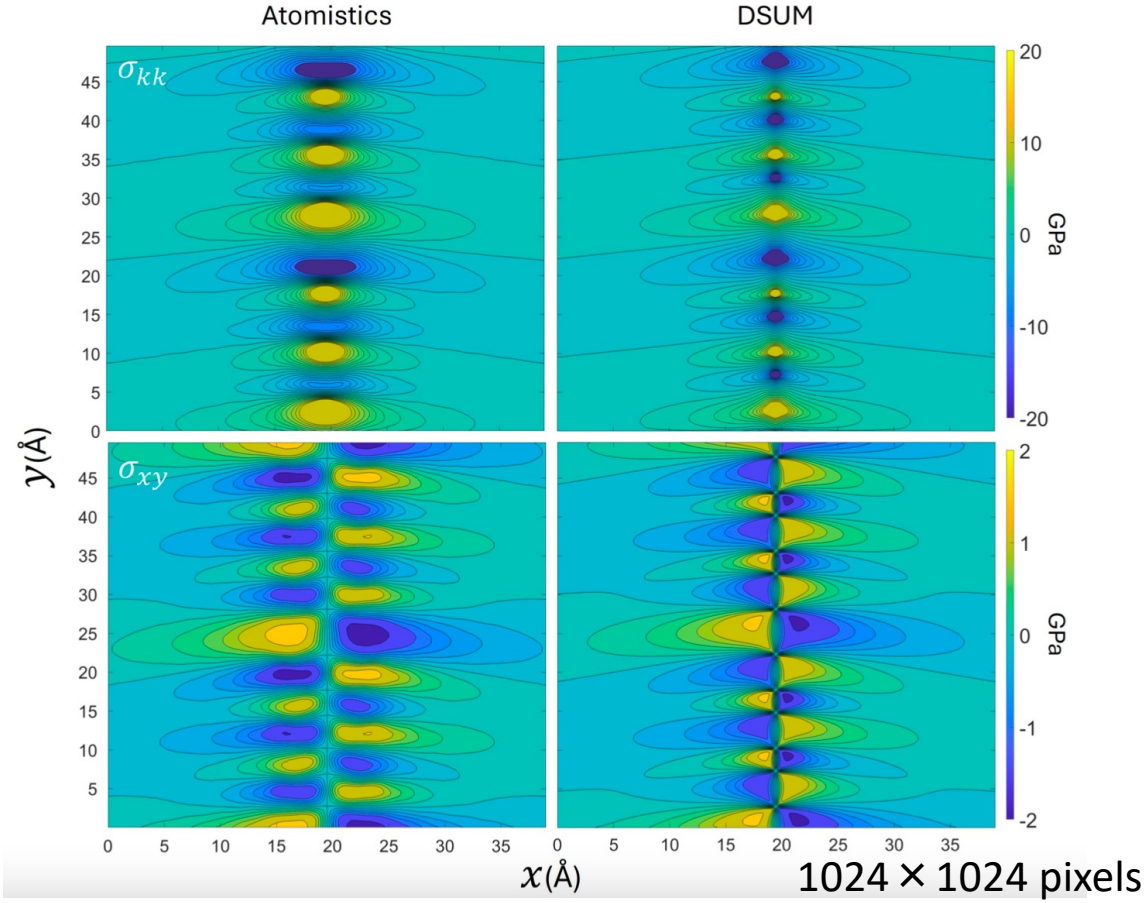
$$\pm\omega = \pm\left(\theta_n - \theta_m\right) = \pm 16.26°$$



$$H = 4L_m + 3L_n$$

Σ149 (10 7 0) [001] 20.02°

Wazne, Petrazoller, Guénolé, Richeton, Berbenni, *submitted (2025)*



Atomistic vs. Anisotropic FFT Ag

$$\omega = \omega_3 = \int_S \theta_{33} dS$$

$$\theta_{33} = \pm \frac{\omega}{2\pi\sigma^2} exp\left(-\frac{r^2}{2\sigma^2}\right) \quad \text{if } r < d$$

$$\theta_{33} = 0 \quad \text{if } r \geq d$$

- Kinematics of dislocations and disclinations and Elasto-statics equations for heterogeneous media
- FFT-numerical resolution and some applications
- **Mesoscopic Field Dislocation Mechanics (MFDM)**
- Numerical implementation based on an elastoviscoplastic FFT scheme (MFDM-EVPFFT)
- Applications of MFDM-EVPFFT
- Summary and outlook

Field Dislocation Mechanics theory equations

- Lattice incompatibility (Nye tensor)

$$\begin{cases} \boldsymbol{\alpha} = \mathbf{curl}(\mathbf{U}_e) \\ \mathbf{div}\ \boldsymbol{\alpha} = \mathbf{0} \end{cases}$$

Discontinuity of displacement along a Burgers circuit C (closed surface S): Burgers vector **b** (multi-valued displacement)

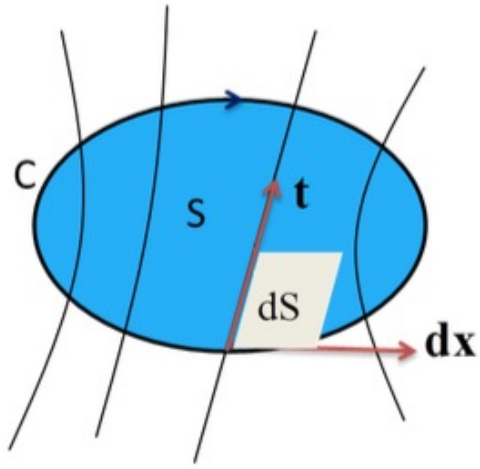
$$\left[\mathbf{u}\right] = \mathbf{b} = \int_C \mathbf{U}_e \mathbf{dx} = \int_S \mathbf{curl}\mathbf{U}_e \cdot \mathbf{n}\, \mathbf{dS} = \int_S \boldsymbol{\alpha} \cdot \mathbf{n}\, \mathbf{dS}$$

E. Kröner, 1958, 1981

- Stress equilibrium (without body force)

$$\mathbf{div}\ \mathbf{T} = \mathbf{0}$$

$$\mathbf{T} = \mathbf{C} : \left\{\mathbf{U}_e\right\} = \mathbf{C} : \boldsymbol{\varepsilon}^e$$



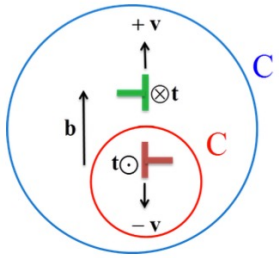
- Dislocation density evolution equation

from Burgers vector conservation, Balance of dislocation flux across an elementary surface

$$\dot{\boldsymbol{\alpha}} = -\mathbf{curl}\left(\boldsymbol{\alpha} \times \mathbf{v}\right) \quad \text{with} \quad \mathbf{v} = \mathbf{f}(\boldsymbol{\alpha}, \mathbf{T})$$

Mura, Phil Mag. 1963, 1964; Acharya 2001

Mesoscopic Field Dislocation Mechanics



- **Evolution of plastic distortion:** $\dot{\mathbf{U}}^{\mathbf{p}} = \boldsymbol{\alpha} \times \mathbf{v} + \mathbf{L}^{\mathbf{p}}$

  $\mathbf{L}^{p} = \overline{(\boldsymbol{\alpha} - \overline{\boldsymbol{\alpha}}) \times \mathbf{v}} = \overline{\boldsymbol{\alpha} \times \mathbf{v}} - \overline{\boldsymbol{\alpha}} \times \overline{\mathbf{v}}$

  Acharya et Roy, 2006

- **SSD (Statistically stored dislocations) and Crystal plasticity:**

$$\mathbf{L}^{p} = \sum_{s=1}^{N} \dot{\gamma}^{s} \mathbf{m}^{s} \otimes \mathbf{n}^{s} \quad \text{with} \quad \dot{\gamma}^{s} = \dot{\gamma}^{0} \left(\left| \tau^{s} \right| / \hat{\tau}_{c} \right)^{1/m} \operatorname{sign}\left(\tau^{s} \right)$$

- **GND (Geometrically Necessary Dislocation) density transport equation**

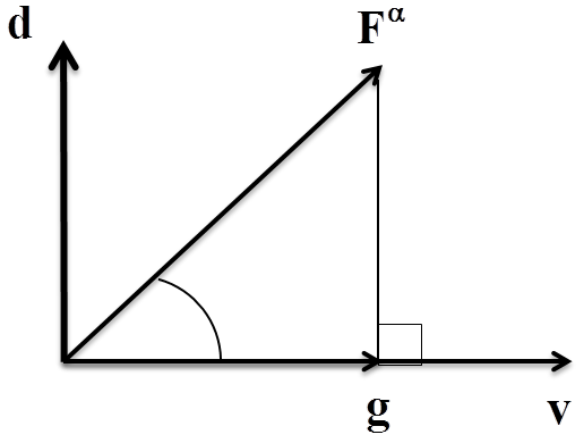
$$\dot{\boldsymbol{\alpha}} = -\mathbf{Curl}\left(\boldsymbol{\alpha} \times \mathbf{v} + \mathbf{L}^{\mathbf{p}} \right) \qquad F_{l}^{\alpha} = e_{ikl} \sigma_{ij} \alpha_{jk}$$

- **Intrinsic Dissipation** $\mathbf{D} = \int_{V} \boldsymbol{\sigma} : \mathbf{L}^{\mathbf{p}} \, \mathbf{dV} + \int_{V} \mathbf{F}^{\boldsymbol{\alpha}} \cdot \mathbf{v} \, \mathbf{dV}$ with: $\mathbf{F}^{\boldsymbol{\alpha}} = \boldsymbol{X} : \boldsymbol{\sigma} \cdot \boldsymbol{\alpha}$
  - **Constitutive equations (GNDs)**

$$\mathbf{v} = \frac{\mathbf{g}}{|\mathbf{g}|} \overline{\mathrm{v}} \quad \overline{\mathrm{v}} \geq 0$$

$$\mathbf{g} = \mathbf{F}^{\alpha} - \left(\mathbf{F}^{\alpha} . \frac{\mathbf{d}}{|\mathbf{d}|} \right) \frac{\mathbf{d}}{|\mathbf{d}|}$$

$$\overline{\mathrm{v}} = \frac{\eta^{2} \, \mathrm{b}}{\mathrm{N}} \left(\frac{\mu}{\hat{\tau}_{c}} \right)^{2} \sum_{s=1}^{N} \left| \dot{\gamma}^{s} \right|$$



$\mathbf{g}$: glide force **X**: Levi-Civita

$\mathbf{F}^{\alpha}$: Peach-Koehler driving force

$\mathbf{d}$: dilatant direction

$\overline{\mathrm{v}}$: GND velocity magnitude

η : materials parameter

N : number of slip systems here N=12 for fcc metals (111)<110>

- **Interfacial jump condition:** $\left[\dot{\mathbf{U}}^{\mathbf{p}} \right] \times \mathbf{n} = \mathbf{0}$ $\mathbf{n}$: interfacial unit vector *Acharya 2007*

Crystal plasticity-based strain-hardening models

MFDM-EVP-FFT vs. Conventional Crystal Plasticity (CP-EVP-FFT)

- **Crystal Plasticity (CP-EVP-FFT) :** no hardening due to GNDs (classic incremental Voce law, hardening due to SSDs) (Kocks et al. 1976, Kalidindi et al 1992, ..)

$$\dot{\hat{\tau}}_c = \theta_0 \frac{\tau_s - \hat{\tau}_c}{\tau_s - \tau_0} \dot{\Gamma} \quad \text{with } \dot{\Gamma} = \sum_{s=1}^{12} \left| \dot{\gamma}^{(s)} \right|$$

- **Mesoscale FDM crystal plasticity (MFDM-EVP-FFT)**: hardening due to GNDs and SSDs (in a Voce type law) (extension of Mecking-Kocks 1981, see Acharya-Beaudoin 2000, …)

$$\dot{\hat{\tau}}_c = \theta_0 \frac{\tau_s - \hat{\tau}_c}{\tau_s - \tau_0} \dot{\Gamma} + k_0 \frac{\eta^2 \mu^2 b}{2\left(\hat{\tau}_c - \tau_0\right)} \sum_{s=1}^{12} \left| \boldsymbol{\alpha} \cdot \mathbf{n}^{(s)} \right| \left| \dot{\gamma}^{(s)} \right| + k_0 \frac{\eta^2 \mu^2 b}{2\left(\hat{\tau}_c - \tau_0\right)} \sum_{s=1}^{12} \left| \boldsymbol{\alpha} \cdot \mathbf{n}^{(s)} \right| \left| \boldsymbol{\alpha} \times \mathbf{V} \right|$$

$$\text{with } \dot{\Gamma} = \left| \boldsymbol{\alpha} \times \mathbf{V} \right| + \sum_{s=1}^{12} \left| \dot{\gamma}^{(s)} \right| \quad \text{and} \quad L_g = \frac{1}{k_0 \left| \boldsymbol{\alpha} \cdot \mathbf{n}^{(s)} \right|}$$

« geometric » (physical) mean free path

- Kinematics of dislocations and disclinations and Elasto-statics equations for heterogeneous media
- FFT-numerical resolution and some applications
- Mesoscopic Field Dislocation Mechanics (MFDM)
- **Numerical implementation based on an elastoviscoplastic FFT scheme (MFDM-EVPFFT)**
- Applications
- Summary and outlook

EVP-FFT formulation with Augmented Lagrangian scheme

- **Elasto-viscoplastic constitutive law (implicit backward Euler time integration)**

$$\boldsymbol{\varepsilon}^{t+\Delta t} = \mathbf{C}^{-1} : \mathbf{T}^{t+\Delta t} + \boldsymbol{\varepsilon}^{p,t} + \dot{\boldsymbol{\varepsilon}}^{p,t+\Delta t}(\mathbf{T}^{t+\Delta t})\Delta t$$ *Lebensohn et al. IJP (2012)*

- **Lippmann-Schwinger integral equation**

$$\boldsymbol{\varepsilon}(\mathbf{x}) = \mathbf{E} - \left(\boldsymbol{\Gamma}^0 * \boldsymbol{\tau}\right)(\mathbf{x}) \quad \text{with} \begin{cases} \tau_{ij} = \delta C_{ijkl}\varepsilon_{kl} & \text{: stress polarization tensor} \\ \Gamma^0_{ijkl} & \text{: modified Green tensor} \end{cases}$$

$$\xrightarrow{\text{FFT}} \quad \tilde{\boldsymbol{\varepsilon}}(\boldsymbol{\xi}) = -\boldsymbol{\Gamma}^0(\boldsymbol{\xi}) : \boldsymbol{\tau}(\boldsymbol{\xi}) \quad \text{and} \quad \tilde{\boldsymbol{\varepsilon}}(0) = \mathbf{E}$$

- **Solved by Augmented Lagrangian formulation (non linear)** *Michel et al., IJNME (2001)*
- **To avoid spurious oscillations: Finite difference schemes together with DFT**
  Willot CRM (2015); Berbenni et al., IJSS (2014); Djaka et al. CMAME (2017)
- **Spectral resolution of GND density transport:**

Hyperbolic transport equation Exponential spectral filter (*Djaka et al, MSMSE 2015*)

$$\tilde{\alpha}_{ij}^{t+\Delta t} = \sigma(\eta)\left[\tilde{\alpha}_{ij}^{t} - \Delta t\, i\, \xi_k \left[\widetilde{(\alpha_{ij} v_k)}^{t} - \widetilde{(\tilde{\alpha}_{ik}\tilde{v}_j)}^{t}\right]\right] - \Delta t\, i\, \xi_k\, e_{jkl}\widetilde{(L^p_{il})}^{t}$$

$$\sigma\left(\frac{k_1}{N_1}, \frac{k_2}{N_2}, \frac{k_3}{N_3}\right) = \exp\left(-\beta\left(\left(\frac{k_1}{N_1}\right)^{2p} + \left(\frac{k_2}{N_2}\right)^{2p} + \left(\frac{k_3}{N_3}\right)^{2p}\right)\right) \text{ with } \begin{cases} \beta = -\log \varepsilon_M & \text{: « damping » parameter} \\ \varepsilon_M & \text{: relatively small value} \\ \eta & \text{: discrete frequencies} \end{cases} \quad 2p : \text{filter order}$$

This is a hyperbolic Hamilton-Jacobi type equation (see also *Morin et al. MSMSE2019, Upadhyay-Bleyer MSMSE2022,* for Godunov-type, discontinuous Galerkin finite element approaches…)

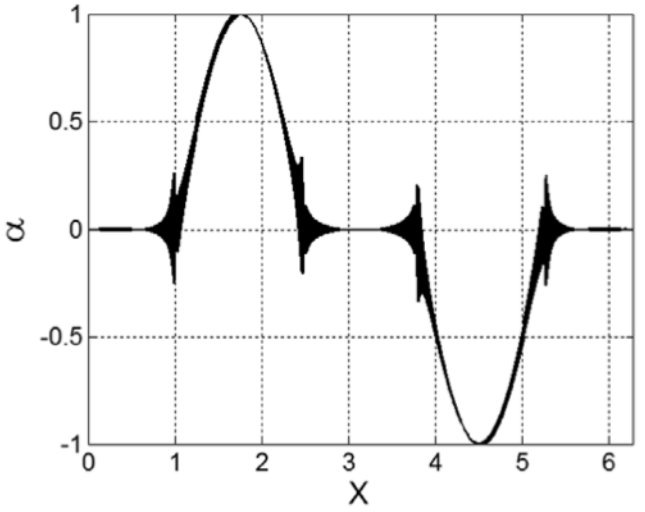
FFT-solver for dislocation density transport equation

$$\dot{\boldsymbol{\alpha}} = -\mathbf{curl}\left(\boldsymbol{\alpha}\times\mathbf{v}\right) \quad \Longrightarrow \quad \alpha_{ij}^{t+\Delta t} = \alpha_{ij}^{t} - \Delta t\left[\left(\alpha_{ij}v_k\right)^t - \left(\alpha_{ik}v_j\right)^t\right]_{,k}$$

- FE-GLS approach (Galerkin Least square method, see *Varadhan et al., 2006*)
- Spectral approach (FFT):

$$\tilde{\alpha}_{ij}^{t+\Delta t} = \left\{\tilde{\alpha}_{ij}^{t} - \Delta t\, i\, \xi_k\left[\widetilde{\left(\alpha_{ij}v_k\right)}^t - \widetilde{\left(\alpha_{ik}v_j\right)}^t\right]\right\}$$

Instabilities due to the PDE hyperbolic character and due to Gibbs oscillations inherent to classic spectral approach



N=1024

Djaka et al. MSMSE 2015

- Filtered spectral approach

$$\tilde{\alpha}_{ij}^{t+\Delta t} = \sigma(\eta)\left\{\tilde{\alpha}_{ij}^{t} - \Delta t\, i\, \xi_k\left[\widetilde{\left(\alpha_{ij}v_k\right)}^t - \widetilde{\left(\alpha_{ik}v_j\right)}^t\right]\right\}$$

Exponential filter $\sigma(\eta) = \exp\left(-\beta(\eta)^{2p}\right)$
(see *Gottlieb-Hesthaven, Spectral methods for hyperbolic problems 2001*)

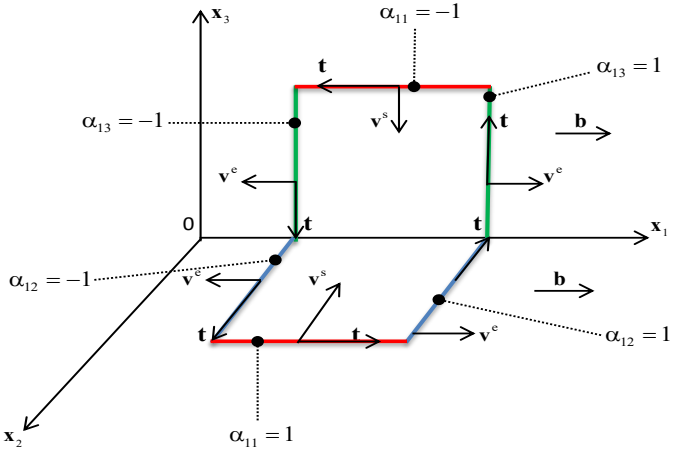
$\beta = -\log \varepsilon_M$: « damping » parameter
ε_M : relatively small value
η : discrete frequencies
$2p$: filter order

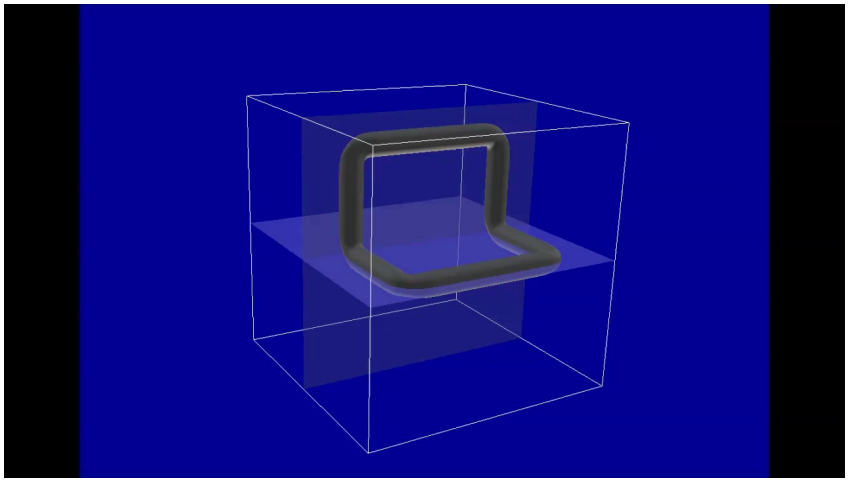
$$\sigma\left(\frac{k_1}{N_1},\frac{k_2}{N_2},\frac{k_3}{N_3}\right) = \exp\left(-\beta\left(\left(\frac{k_1}{N_1}\right)^{2p} + \left(\frac{k_2}{N_2}\right)^{2p} + \left(\frac{k_3}{N_3}\right)^{2p}\right)\right)$$

FFT-solver for dislocation density transport equation: Application to 3D polygonal dislocation loop shrinkage

$$\dot{\alpha} = -\mathbf{curl}\left(\alpha \times \mathbf{v}\right) \Rightarrow \tilde{\alpha}_{ij}^{t+\Delta t} = \sigma(\eta)\left\{\tilde{\alpha}_{ij}^{t} - \Delta t\, i\, \xi_k \left[\widetilde{\left(\alpha_{ij} v_k\right)}^{t} - \widetilde{\left(\alpha_{ik} v_j\right)}^{t}\right]\right\} \qquad \sigma(\eta) = \exp\left(-\beta(\eta)^{2p}\right)$$

$$\beta = -\log \varepsilon_M$$





N_{tot}	CPU time (s)	
	FFT	FE-GLS
32^3	0.032	20.110
64^3	0.081	164.82
128^3	0.590	1354.3
256^3	5.310	/
512^3	56.00	/

Single core, 2.3Ghz i7, 16Go DDR3

Unit cell voxel number $128 \times 128 \times 128$
Smoothing parameter $\varepsilon_M = 0.2$
Fraction of CFL limit: $c = 0.25$
Constant velocity $v_0 = 5 \times 10^8\ s^{-1}$
Simulation 3D periodic domain: $2\pi \times 2\pi \times 2\pi$
Filter order: $2p=2$ $(p=1)$

Djaka et al. MSMSE 2015

$$\Delta t_{CFL} = c\frac{\delta}{\bar{v}_{max}}$$

EVP-FFT formulation with Augmented Lagrangian scheme

- **Elasto-viscoplastic constitutive law (implicit backward Euler time integration)**

$$\boldsymbol{\varepsilon}^{t+\Delta t} = \mathbf{C}^{-1} : \mathbf{T}^{t+\Delta t} + \boldsymbol{\varepsilon}^{p,t} + \dot{\boldsymbol{\varepsilon}}^{p,t+\Delta t}(\mathbf{T}^{t+\Delta t})\Delta t$$

Lebensohn, Kanjarla, Eisenlohr, IJP 2012

- **Lippmann-Schwinger integral equation**

$$\boldsymbol{\varepsilon}(\mathbf{x}) = \mathbf{E} - \left(\boldsymbol{\Gamma}^0 * \boldsymbol{\tau}\right)(\mathbf{x}) \quad \text{with} \quad \begin{cases} \tau_{ij} = \delta C_{ijkl}\varepsilon_{kl} : \text{stress polarization tensor} \\ \Gamma^0_{ijkl} : \text{modified Green tensor} \end{cases}$$

FT

$$\tilde{\boldsymbol{\varepsilon}}(\boldsymbol{\xi}) = -\boldsymbol{\Gamma}^0(\boldsymbol{\xi}) : \boldsymbol{\tau}(\boldsymbol{\xi}) \quad \text{and} \quad \tilde{\boldsymbol{\varepsilon}}(0) = \mathbf{E}$$

- **Solved by Augmented Lagrangian formulation (non linear)**

$$\tau_{ij}^{(n)} = \lambda_{ij}^{(n)} - C^0_{ijkl}e^{(n)}_{kl}$$

Michel et al., 2001

$$R^{es}_{ij}(\mathbf{T}^{(n+1)}) = T^{(n+1)}_{ij} + C^0_{ijmn}\varepsilon^{(n+1)}_{mn}(\mathbf{T}^{(n+1)}) - \lambda^{(n)}_{ij} - C^0_{ijmn}e^{(n+1)}_{mn} = 0$$

$$T^{(n+1,p+1)}_{ij} = T^{(n+1,p)}_{ij} - \left(\left(\partial R^{es}_{ij} / \partial T_{mn}\right)_{\mathbf{T}^{(n+1,p)}}\right)^{-1} R^{es}_{mn}\left(\mathbf{T}^{(n+1,p)}\right)$$

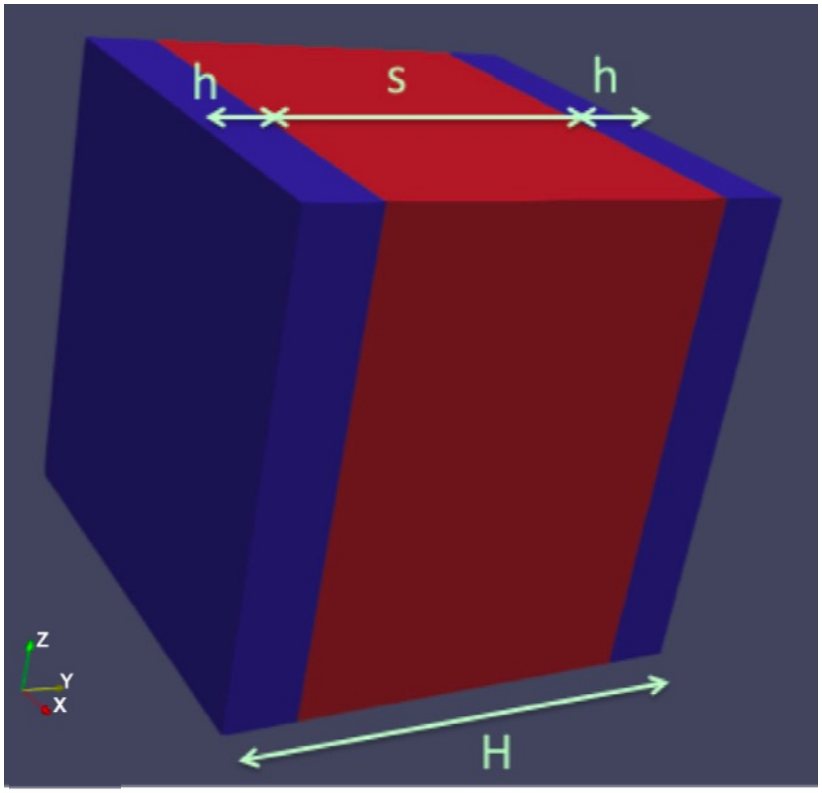
$$\left(\partial R^{es}_{ij} / \partial T_{mn}\right)_{\mathbf{T}^{(n+1,p)}} = \delta_{im}\delta_{jn} + C^0_{ijkl}C^{-1}_{klmn} + \Delta t C^0_{ijkl}\left(\partial \dot{\varepsilon}^p_{kl} / \partial T_{mn}\right)_{\mathbf{T}^{(n+1,p)}}$$

$$\boldsymbol{\lambda}^{(n+1)} = \boldsymbol{\lambda}^{(n)} + \mathbf{C}^0 : \left(\mathbf{e}^{(n+1)} - \boldsymbol{\varepsilon}^{(n+1)}\right)$$ (new guess, Uzawa descent algorithm)

- Kinematics of dislocations and disclinations and Elasto-statics equations for heterogeneous media
- FFT-numerical resolution and some applications
- Mesoscopic Field Dislocation Mechanics (MFDM)
- Numerical implementation based on an elastoviscoplastic FFT scheme (MFDM-EVPFFT)

- **Applications**
- Summary and outlook

Application 1: Two-phase laminate structures



Φ1 (°)	Φ (°)	Φ2 (°)
300.	54.7356	45

- **Simulation parameters**
  - Constant Volume fraction of elastic precipitates: f=0.3125 or f=0.125
  - Period: H=2h+s
  - s: channel size

- **Materials parameters (Al)**

✓ **Isotropic elasticity:** $E = 69\text{GPa} \quad (\mu = 25.9\text{GPa})$, $\nu = 0.33$

✓ **Hardening and flow rule**

$\tau_0 = 3\text{MPa} \qquad \theta_0 = 150\text{MPa}$

$\tau_s = 12\text{MPa} \qquad k_0 = 20 \text{ or } 500$

$b = 2.86 \times 10^{-10}\text{m} \qquad \eta = 0.33$

$\dot{\gamma}_0 = 1\text{s}^{-1} \qquad m = 0.05$

- **Specific parameters for GND density transport equation c: for Courant condition , exponential filter parameters)**

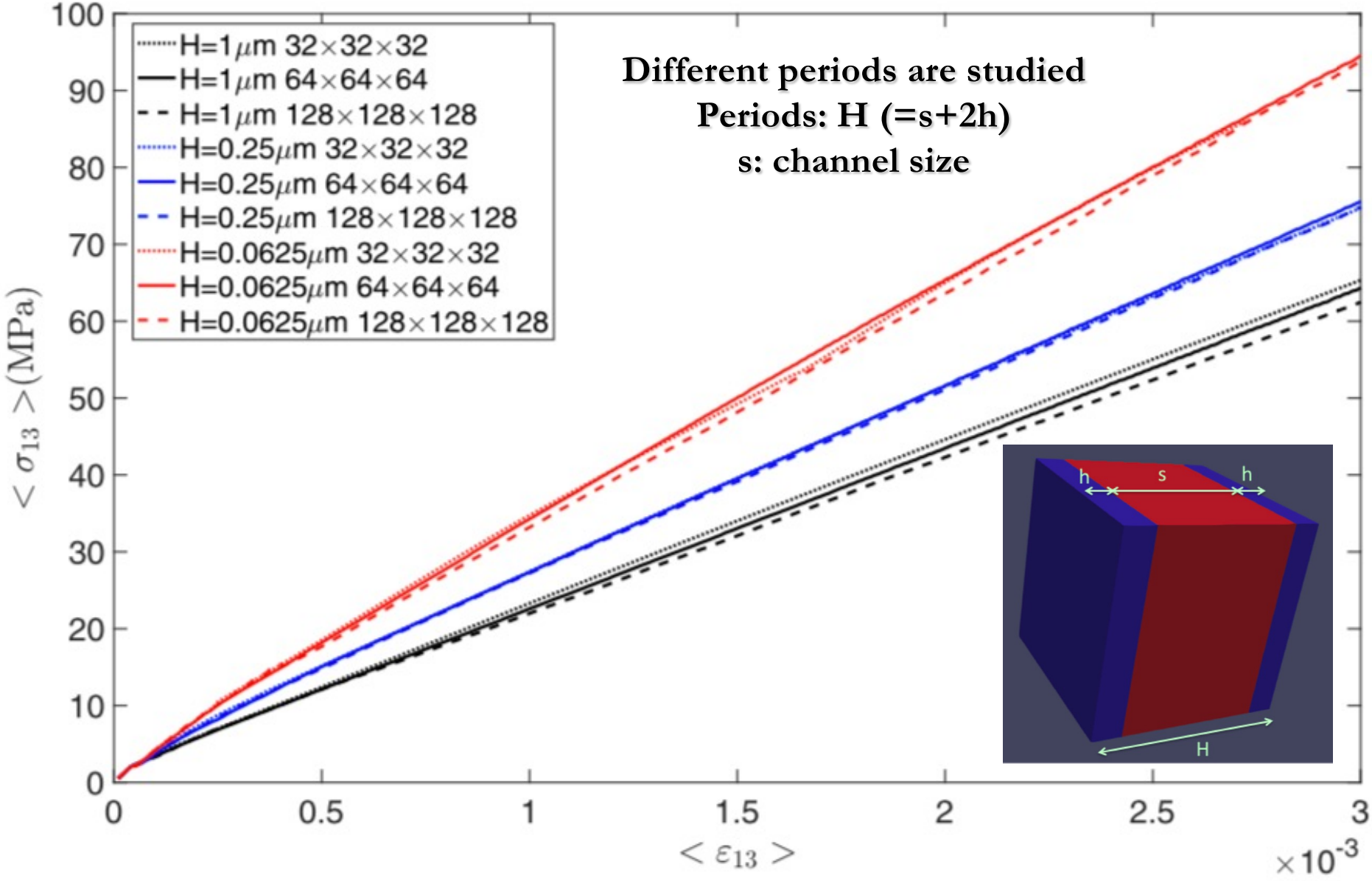
p=1	ε_M=0.2	c=0.25	$\Delta t(\text{CFL}) = \mathbf{c} \cdot \Delta \mathbf{x} / \max(\mathbf{v})$

- **Boundary conditions: Pure shear test**

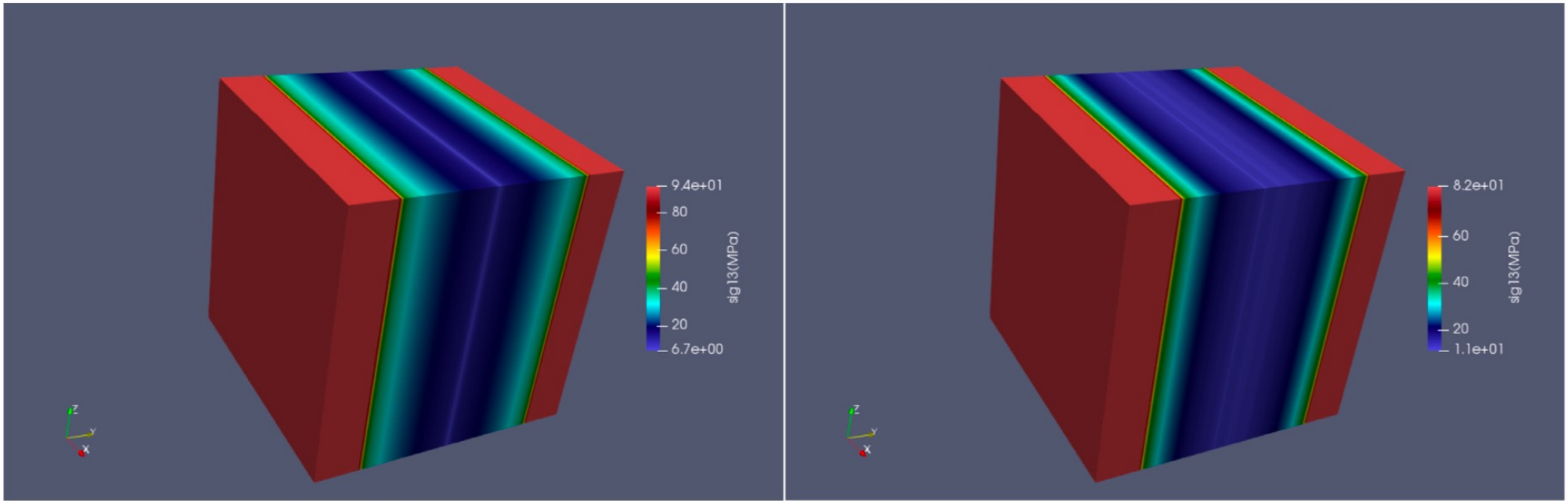
$\dot{E}_{13} = \dot{E}_{31} = 0.001\text{s}^{-1}$

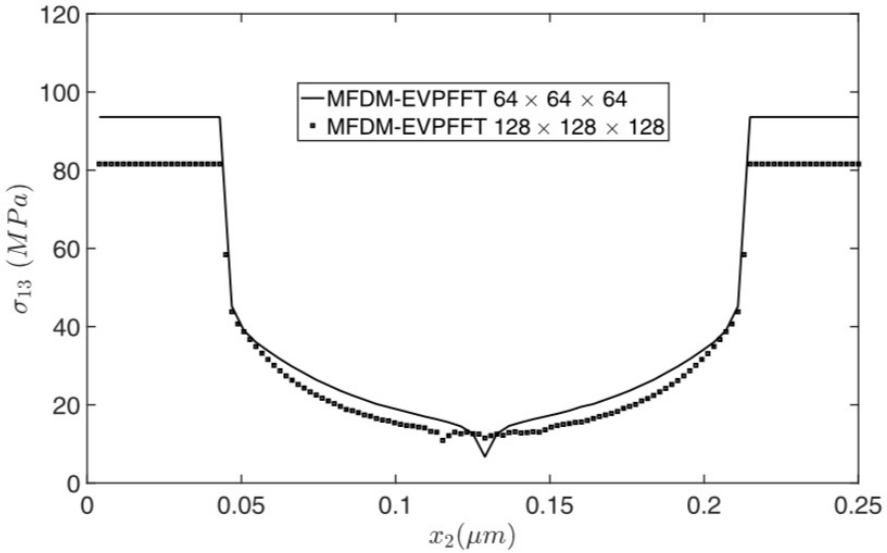
$\Delta t(\text{init}) = 0.01\text{s} \quad \Delta t = \min(\Delta t(\text{init}), \Delta t(\text{CFL}))$

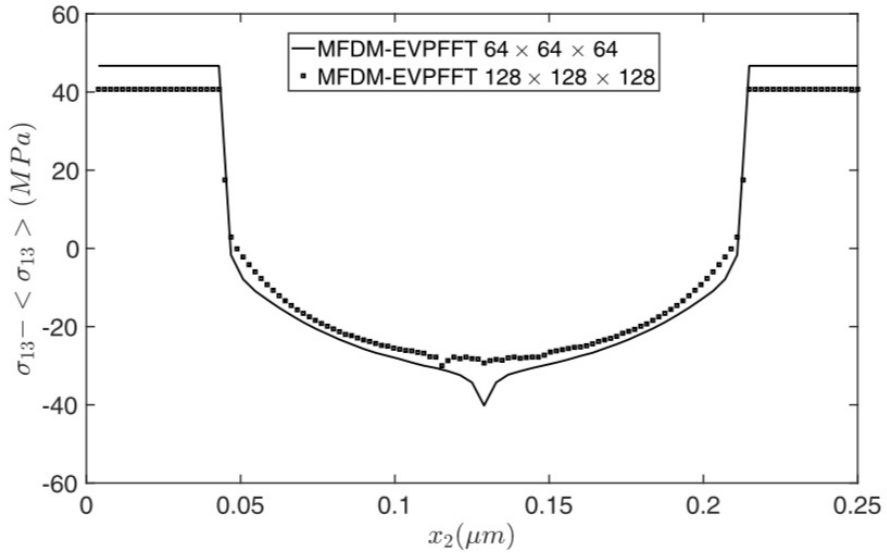
Mesh size convergence



Stress profiles -› spatial gradients

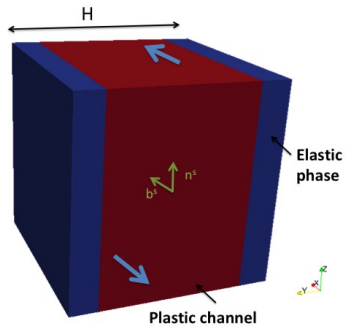






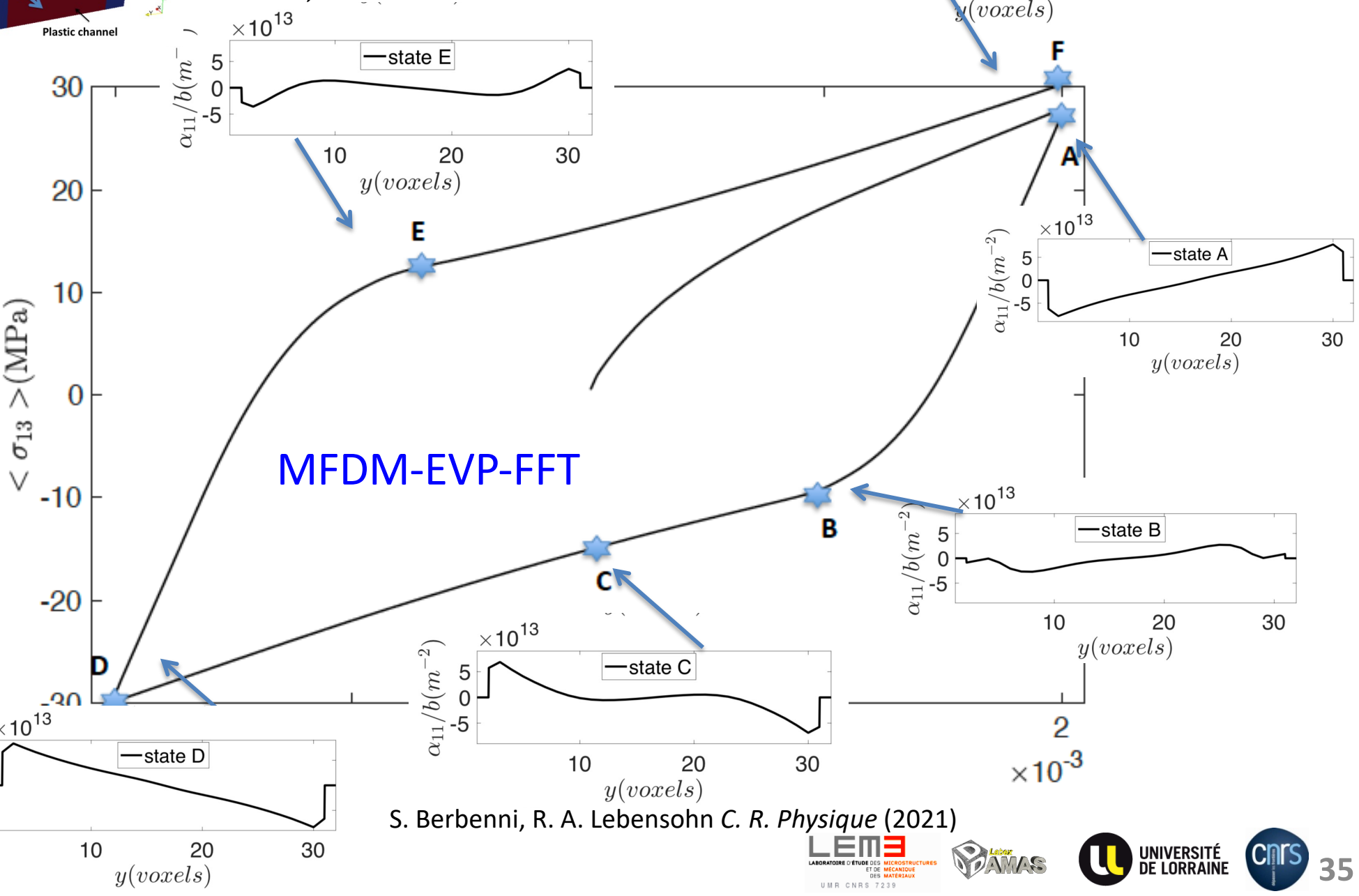
K.S. Djaka, S. Berbenni, V. Taupin, R. A. Lebensohn *Int. J. Solids Struct.* 184 (2020) 136–152

Reversible plas



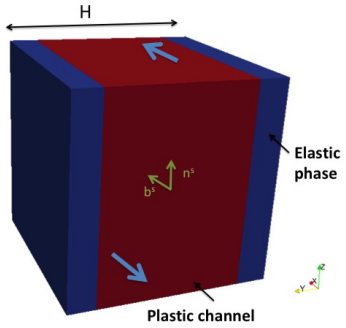
f=0.125

H=0.25µm



S. Berbenni, R. A. Lebensohn *C. R. Physique* (2021)

Reversible plasticity

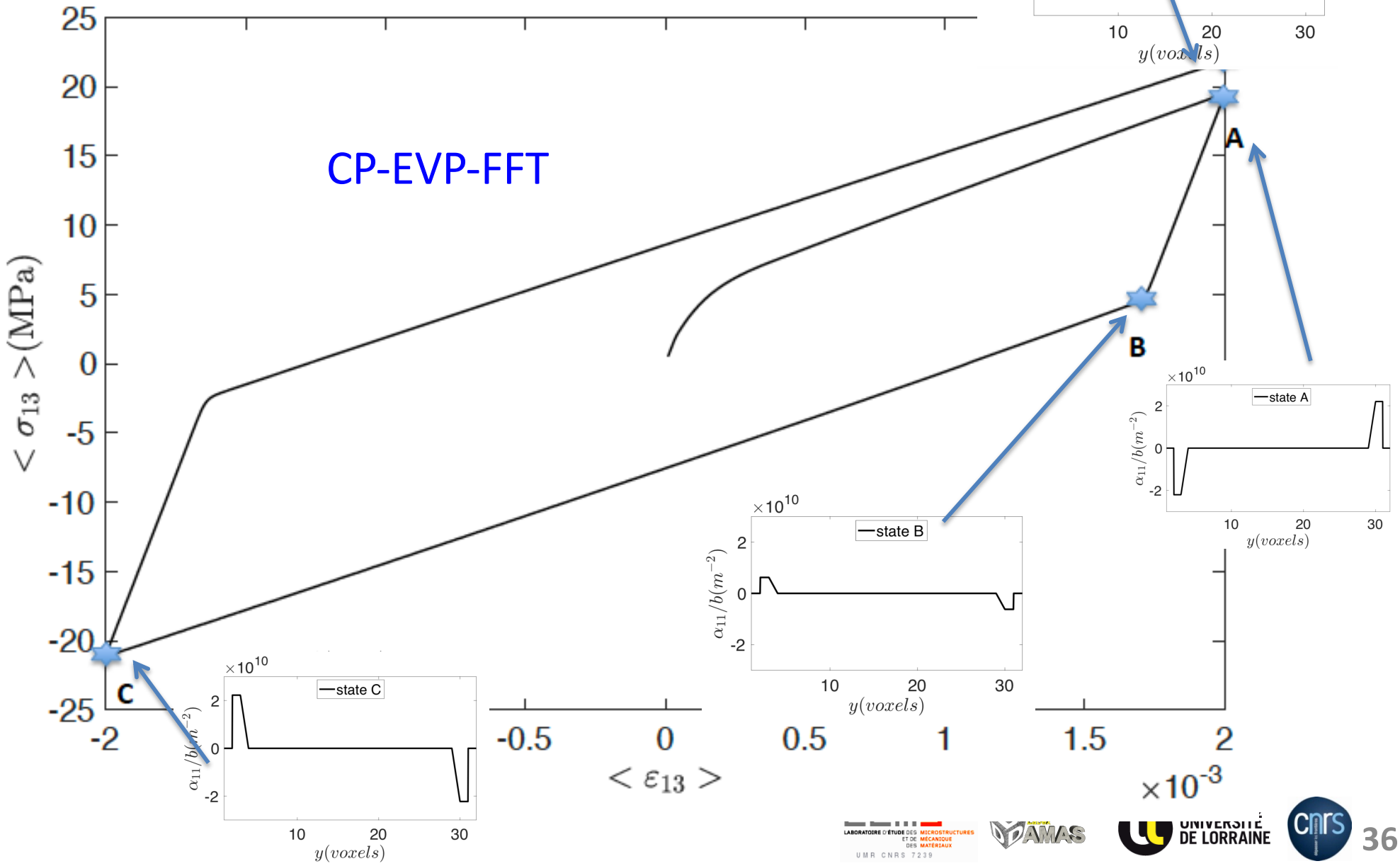


f=0.125

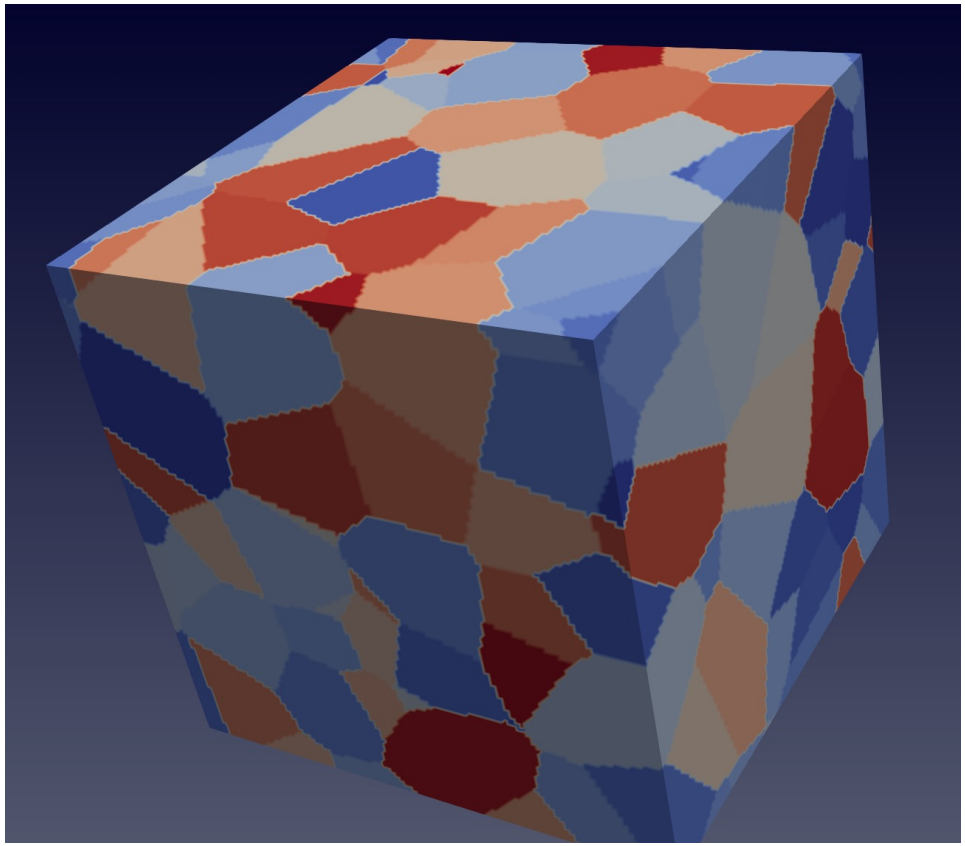
H=0.25µm

Bauschinger effect di
(see Mughrabi) (no s
nly

CP-EVP-FFT



Application 2: Application to F.C.C. polycrystals



Ex: 100 grains (128 × 128 × 128)

- **Simulation parameters**
  - Periodic unit cell: Al polycrystal
  - Random texture
  - 27 grains, Average grain size from 0.083 µm to 125.54 µm ($H/\sqrt[3]{27}$)
  - 100 grains, Average grain size from 0.1 µm to 100 µm ($H/\sqrt[3]{100}$)
- **Materials parameters (Al)**
  - ✓ **Isotropic elasticity**

$$E = 69\text{GPa} \quad (\mu = 25.9\text{GPa}) \qquad \nu = 0.33$$

  - ✓ **Hardening and flow rule**

$$\tau_0 = 3\text{MPa} \quad \theta_0 = 150\text{MPa}$$
$$\tau_s = 12\text{MPa} \quad k_0 = 20$$
$$b = 2.86\times10^{-10}\,\text{m} \quad \eta = 0.33$$
$$\dot{\gamma}_0 = 1\text{s}^{-1} \quad m = 0.05$$

- **Specific parameters for GND density transport equation c: for Courant condition , exponential filter parameters)**

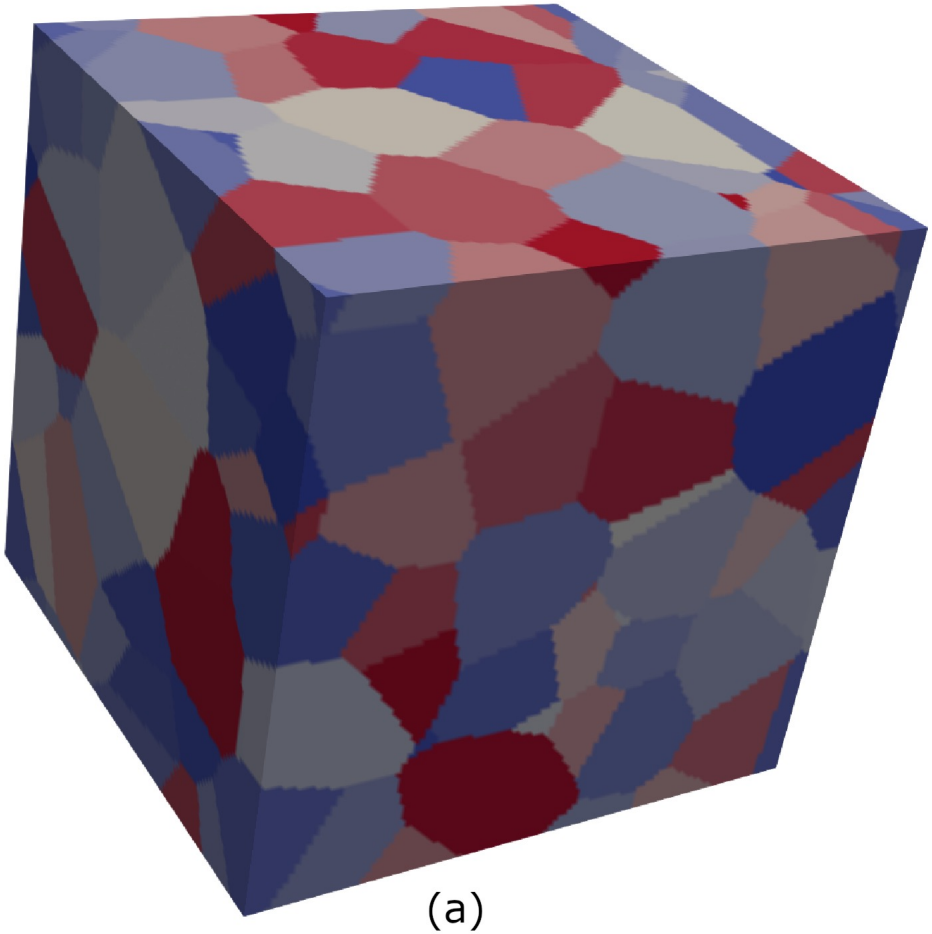
p=1	ε_M=0.2	c=0.25	$\Delta t(\text{CFL}) = \mathbf{c}\cdot\Delta\mathbf{x} / \max(\mathbf{v})$

- **Boundary conditions: Pure tensile test**

$$\dot{E}_{33} = \dot{E}_{33} = 0.001\text{s}^{-1}$$

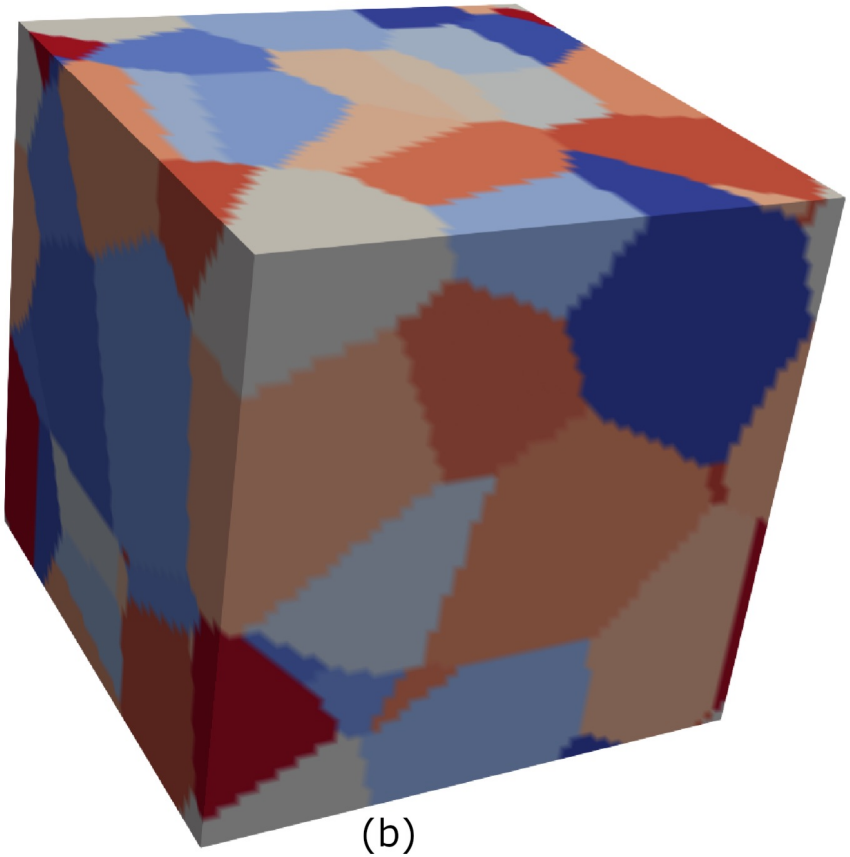
$$\Delta t(\text{init}) = 0.01\text{s} \quad \Delta t = \min(\Delta t(\text{init}), \Delta t(\text{CFL}))$$

Periodic Voronoi tessellated F.C.C. polycrystals



(a)

100 grains (128 × 128 × 128)

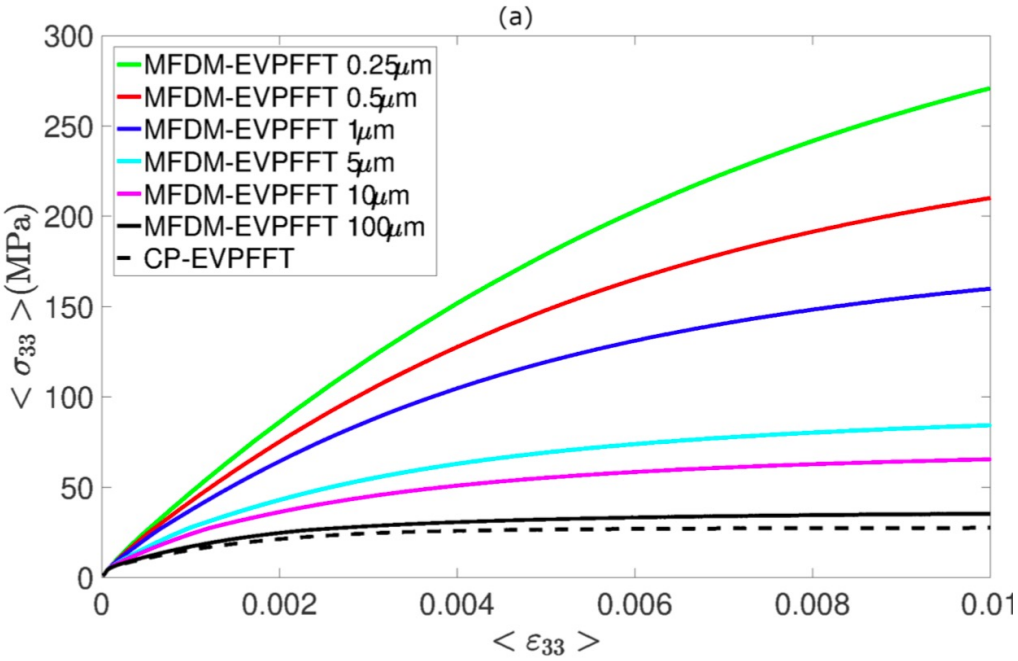


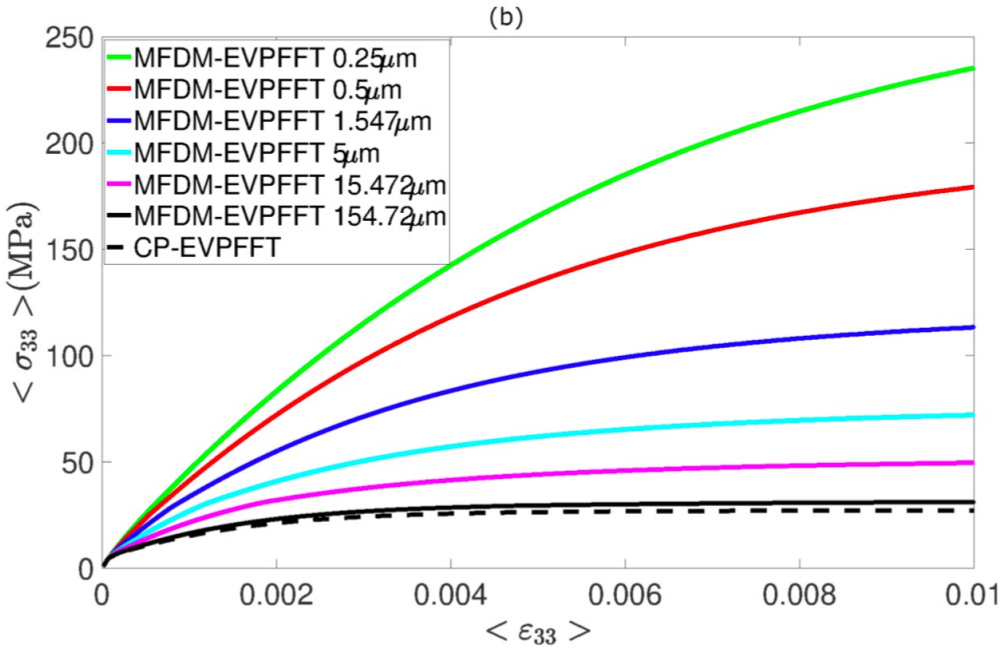
(b)

27 grains (64 × 64 × 64)

S. Berbenni, V. Taupin, R. A. Lebensohn. *Journal of the Mechanics and Physics of Solids* 135 (2020) 103808

Macroscopic tensile stress/strain: Grain size (d) effect (27grains/100 grains in the unit cell)





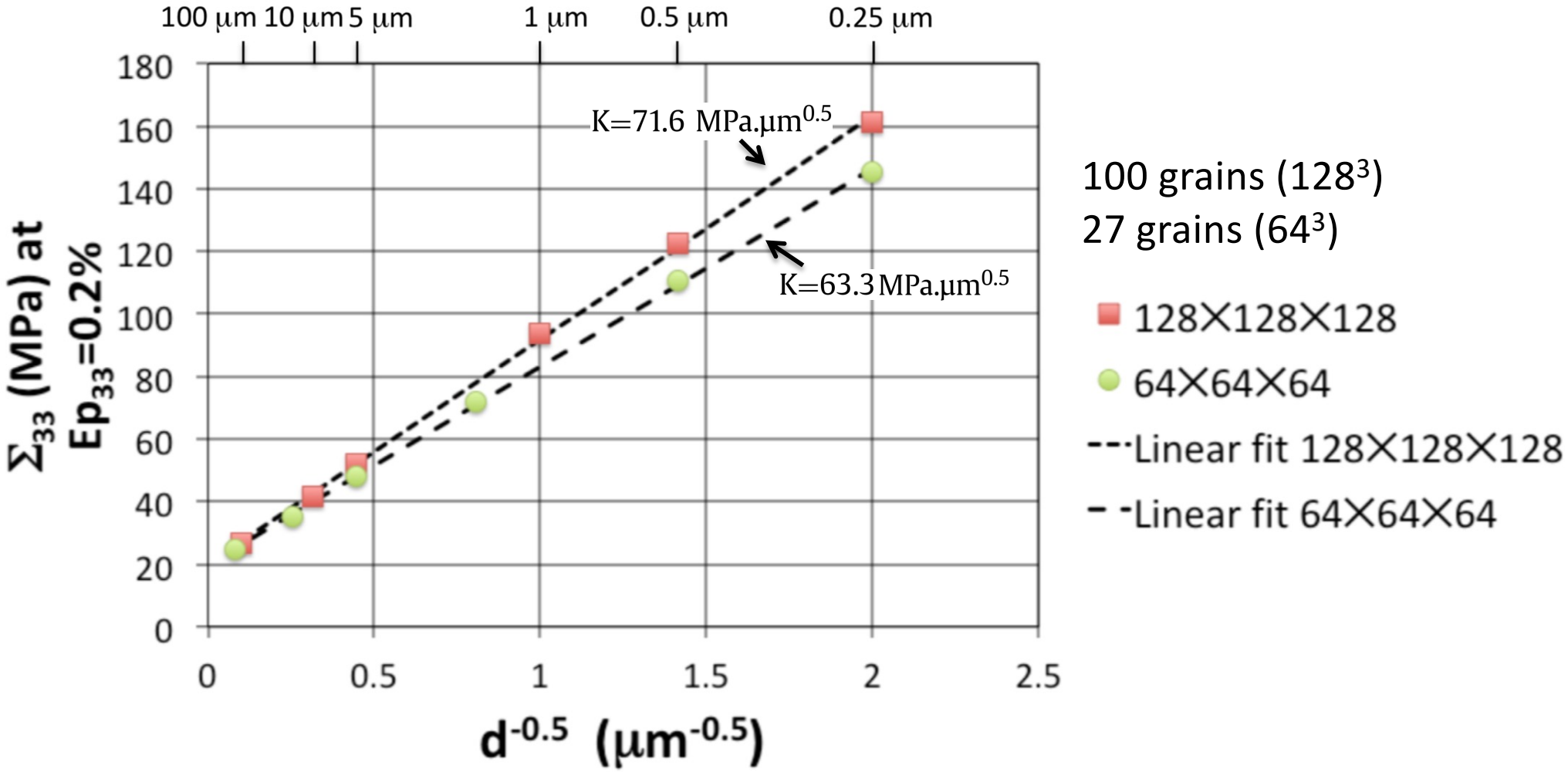
27 grains ($64 \times 64 \times 64$)

100 grains ($128 \times 128 \times 128$)

MFDM-EVP-FFT -> grain size effect

CP-EVP-FFT -> grain size independent

Hall-Petch diagrams (MFDM-EVP-FFT)

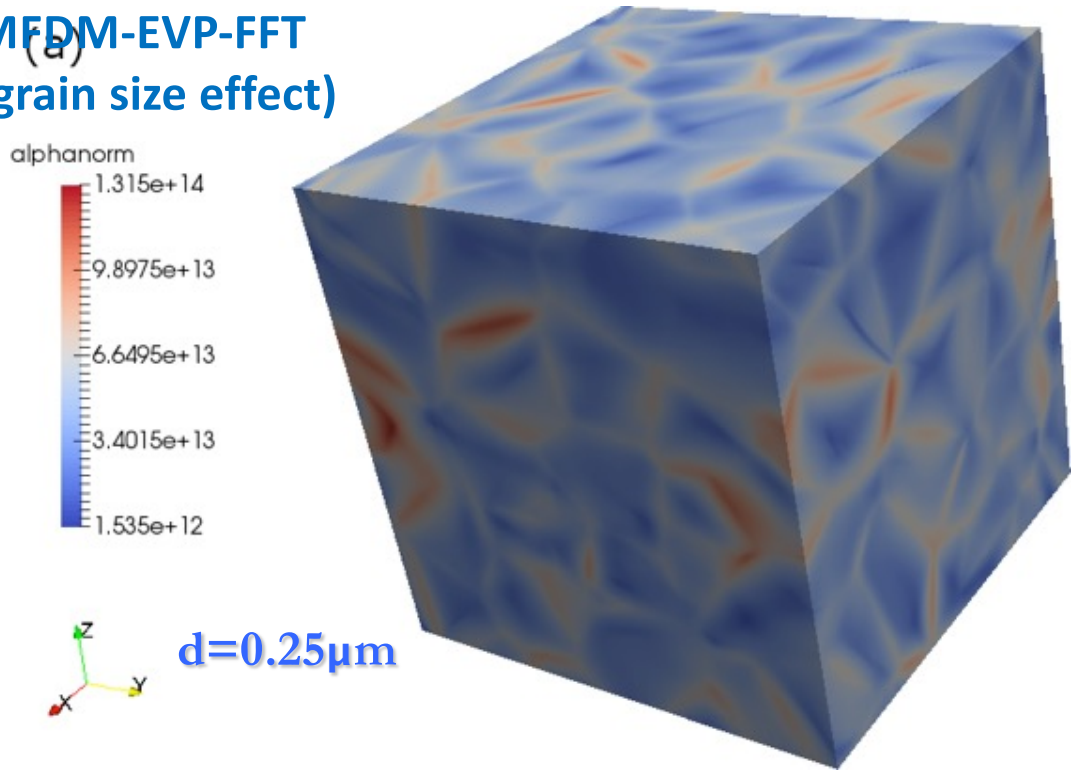


$$< \sigma_{33} >=< \sigma_{33}^{\infty} > + K\bar{d}^{n} \quad \text{with} \quad n = -0.5 \quad < \sigma_{33}^{\infty} >= 19.8\text{MPa}$$

S. Berbenni, V. Taupin, R. A. Lebensohn. *Journal of the Mechanics and Physics of Solids* 135 (2020) 103808

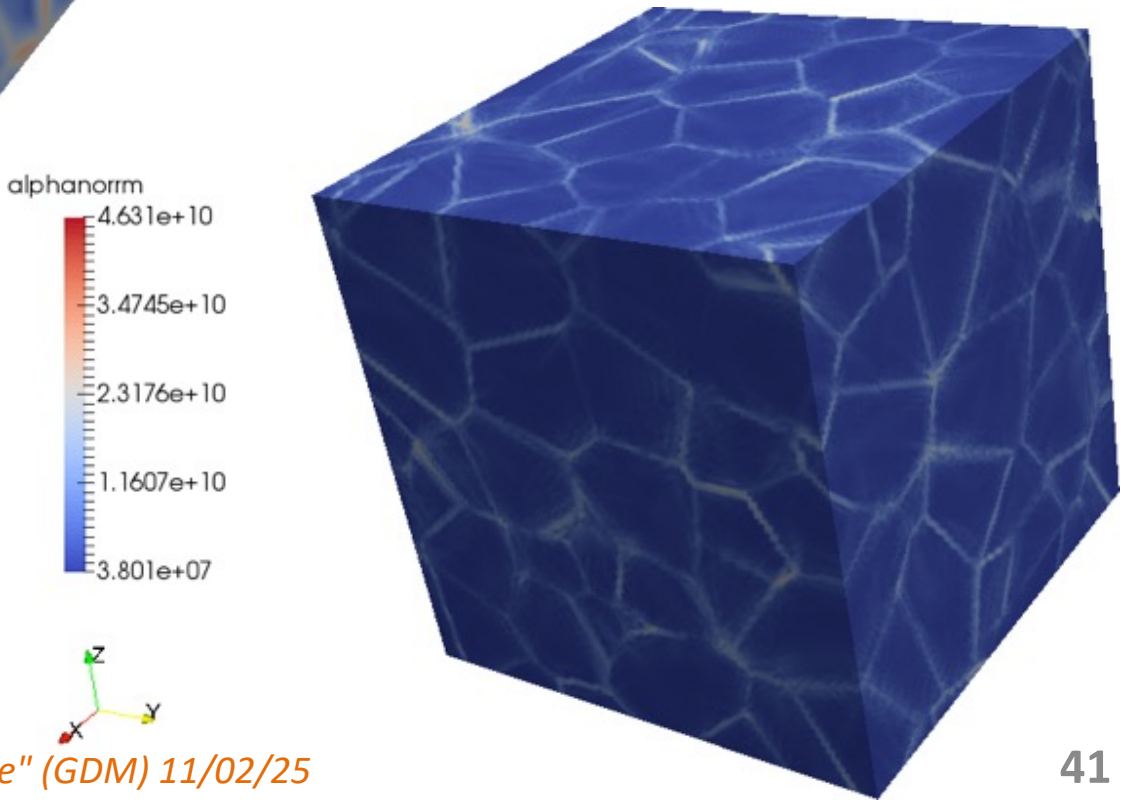
Mesocale Field Dislocation Mechanics in EVP-FFT

MFDM-EVP-FFT
(grain size effect)



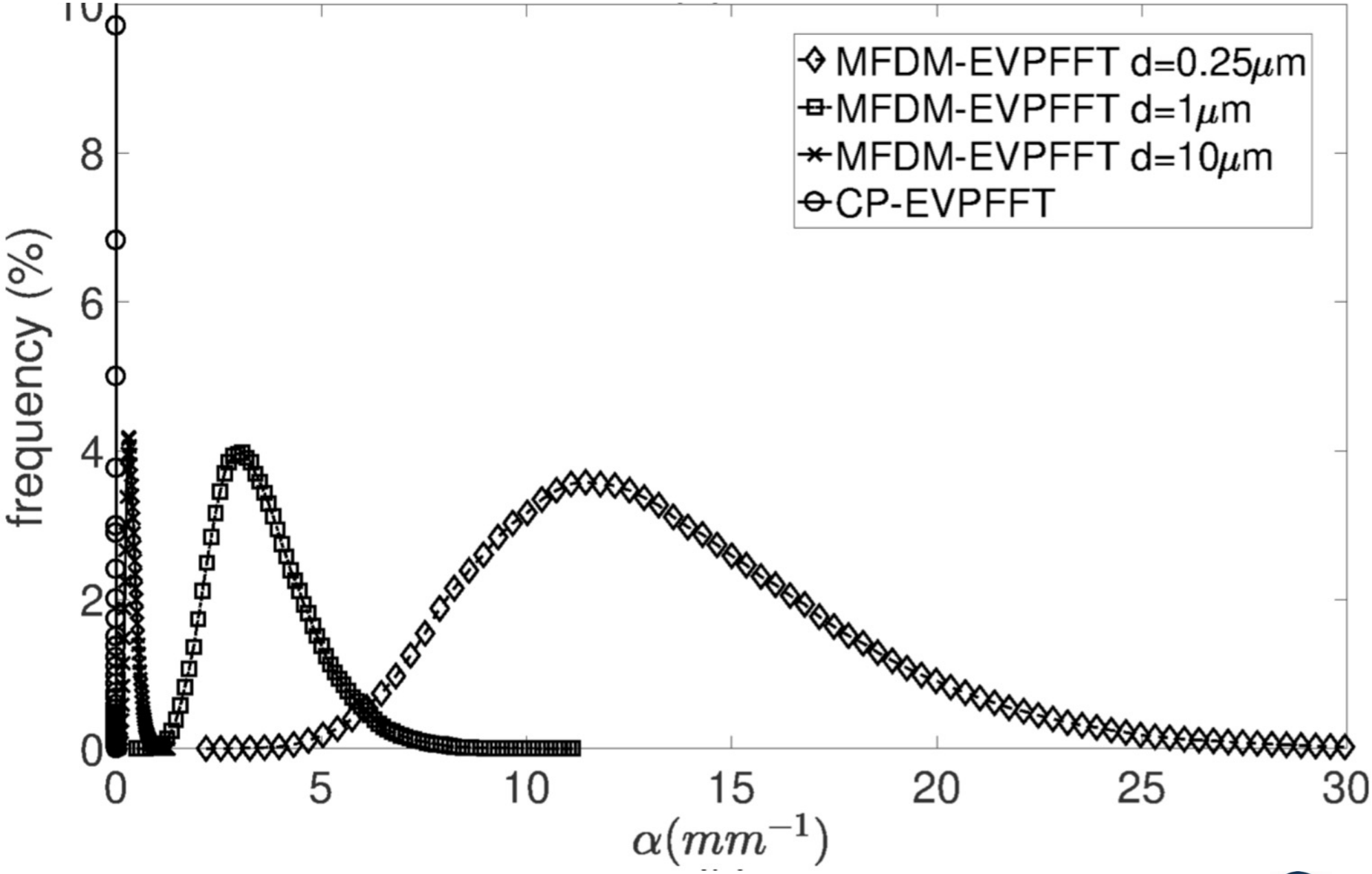
GND density distributions

$$\rho_{GND} = \|\boldsymbol{\alpha}\| / b = \sqrt{\boldsymbol{\alpha} : \boldsymbol{\alpha}} / b$$



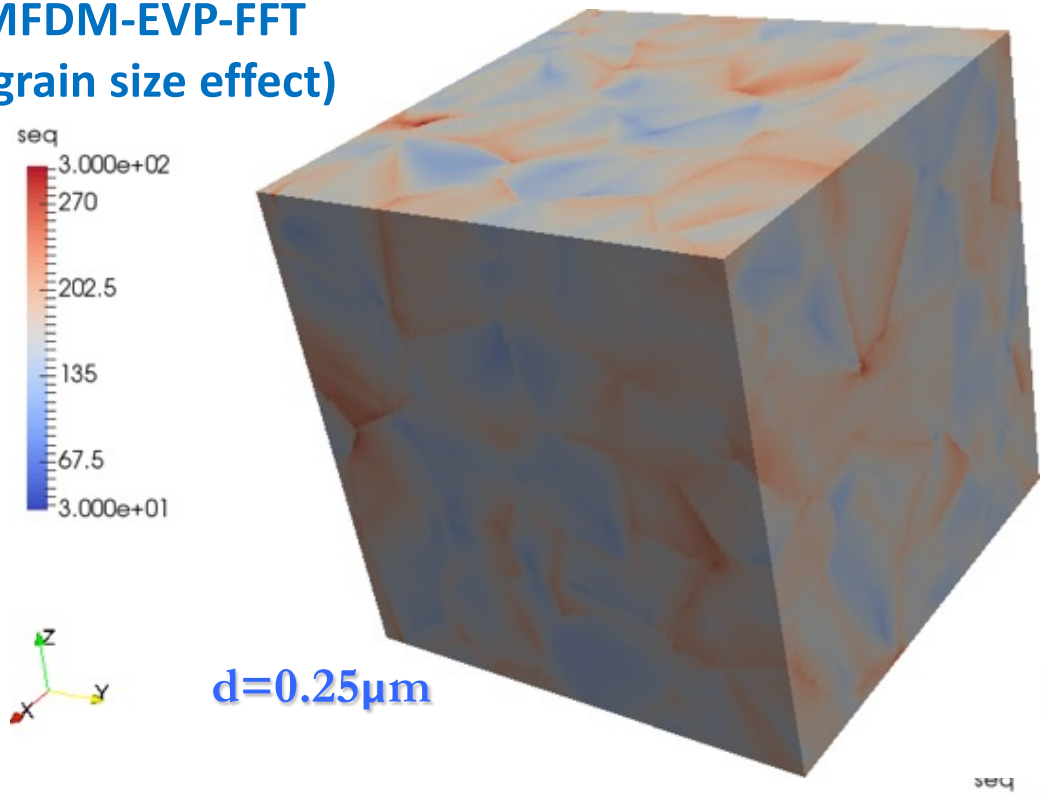
CP-EVP-FFT
(no grain size effect)

Field Histogram



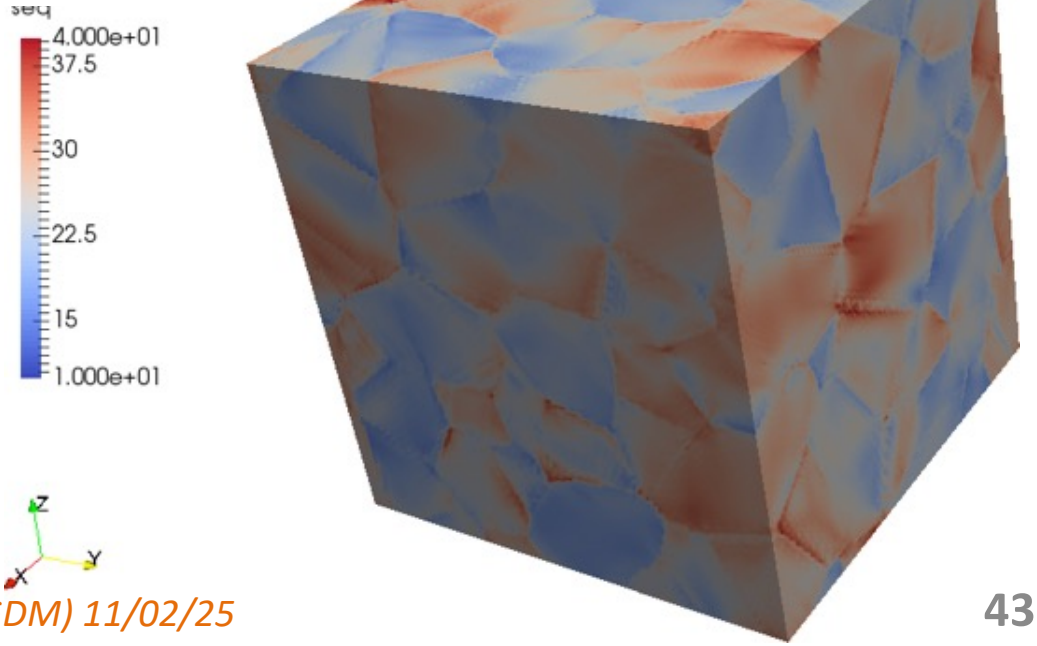
Mesocale Field Dislocation Mechanics in EVP-FFT

MFDM-EVP-FFT
(grain size effect)



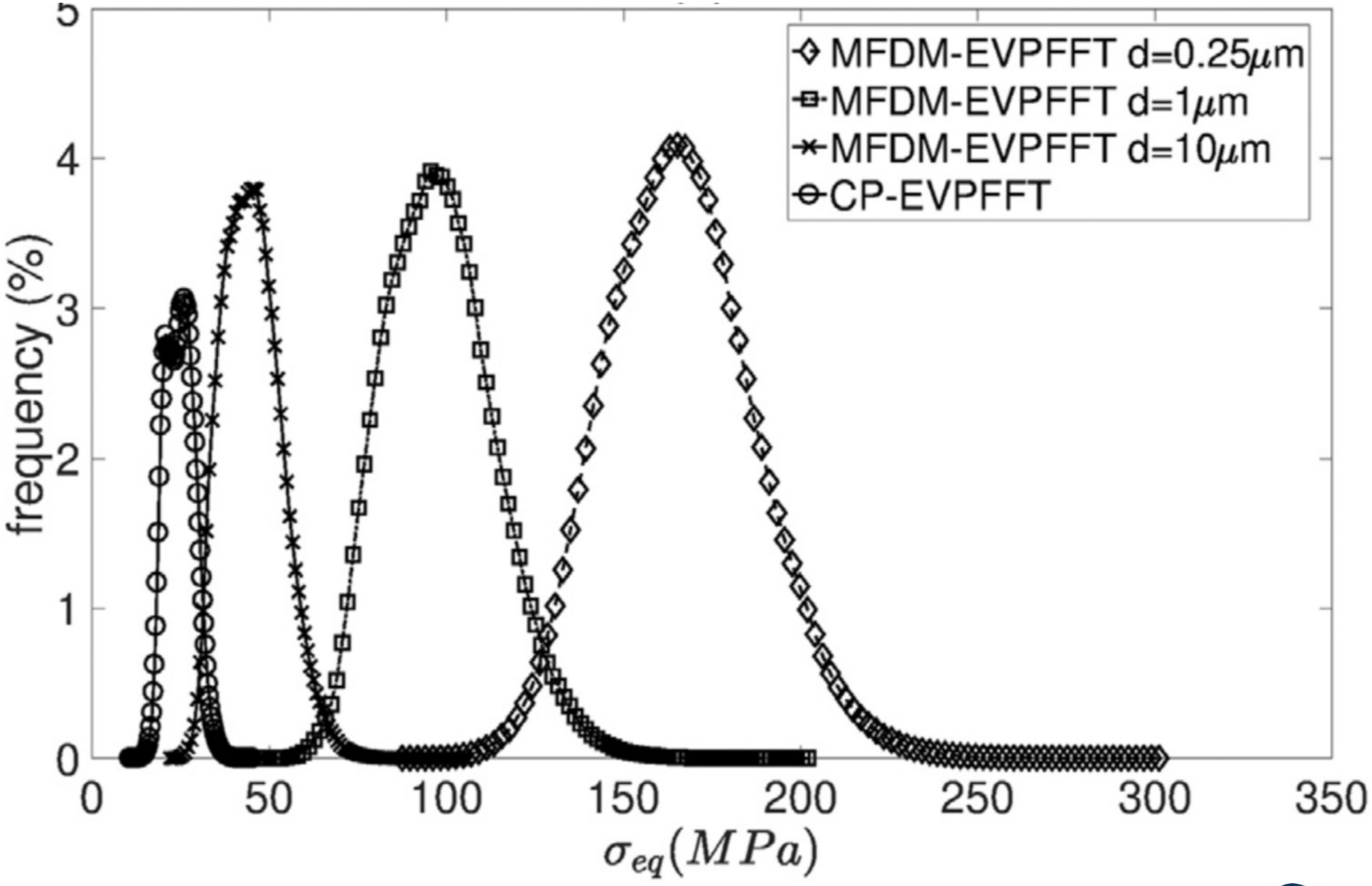
Equivalent Von Mises stress

$$\sigma_{eq} = \sqrt{\frac{3}{2}\mathbf{s}:\mathbf{s}}$$



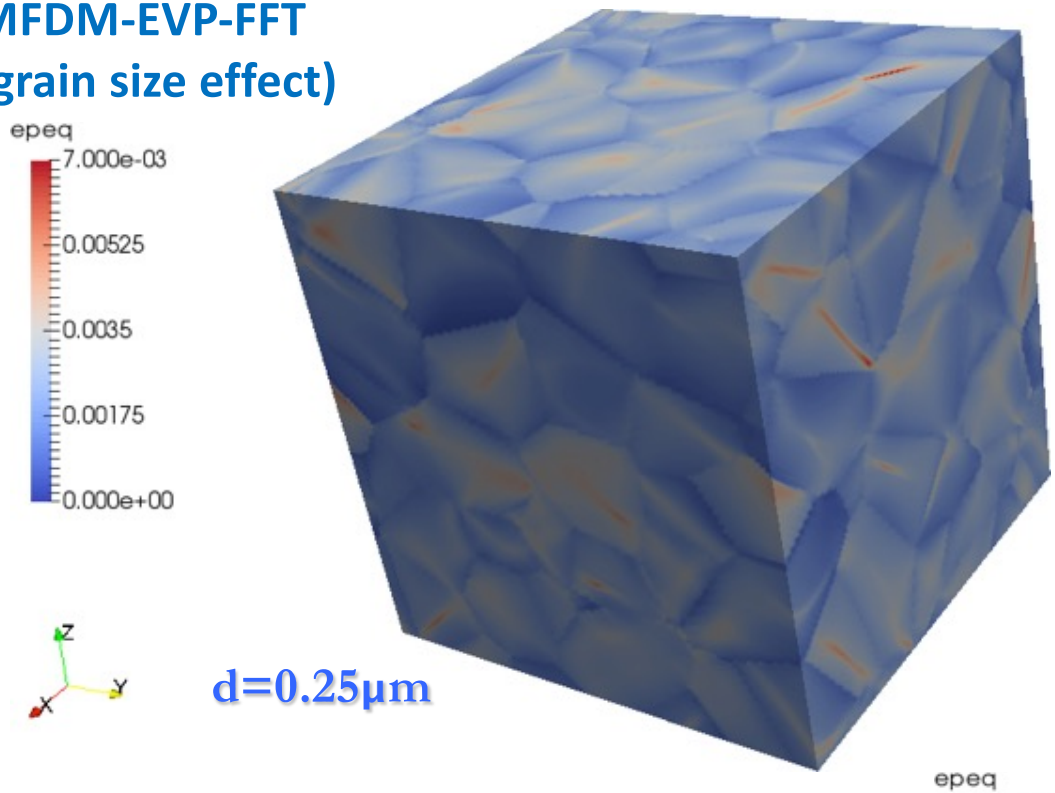
CP-EVP-FFT
(no grain size effect)

Field Histogram



Mesocale Field Dislocation Mechanics in EVP-FFT

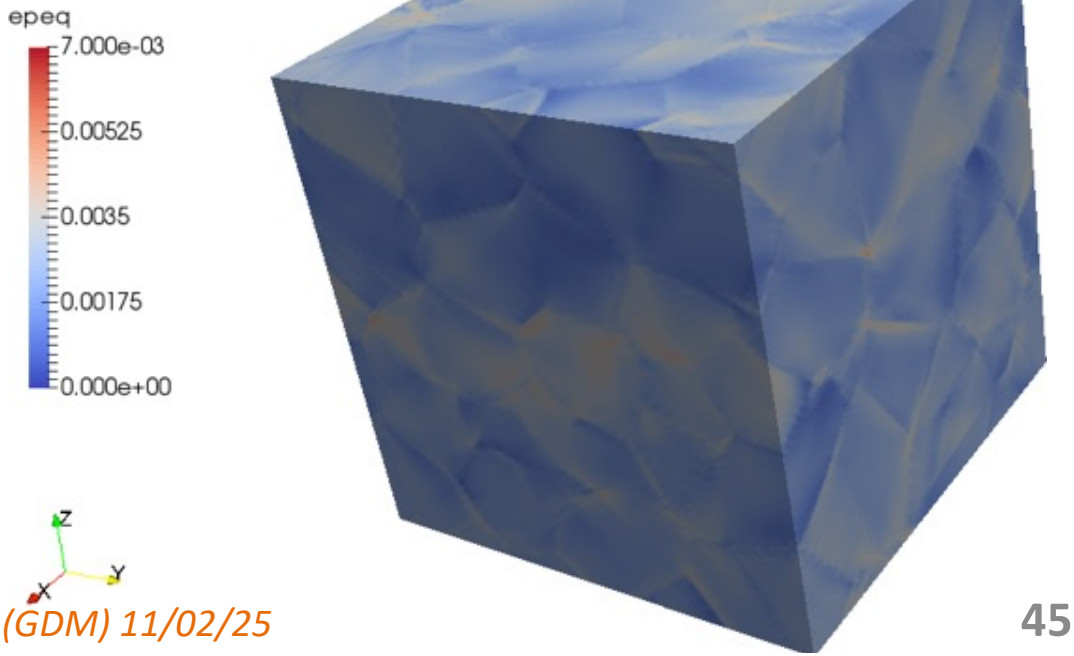
MFDM-EVP-FFT
(grain size effect)



d=0.25µm

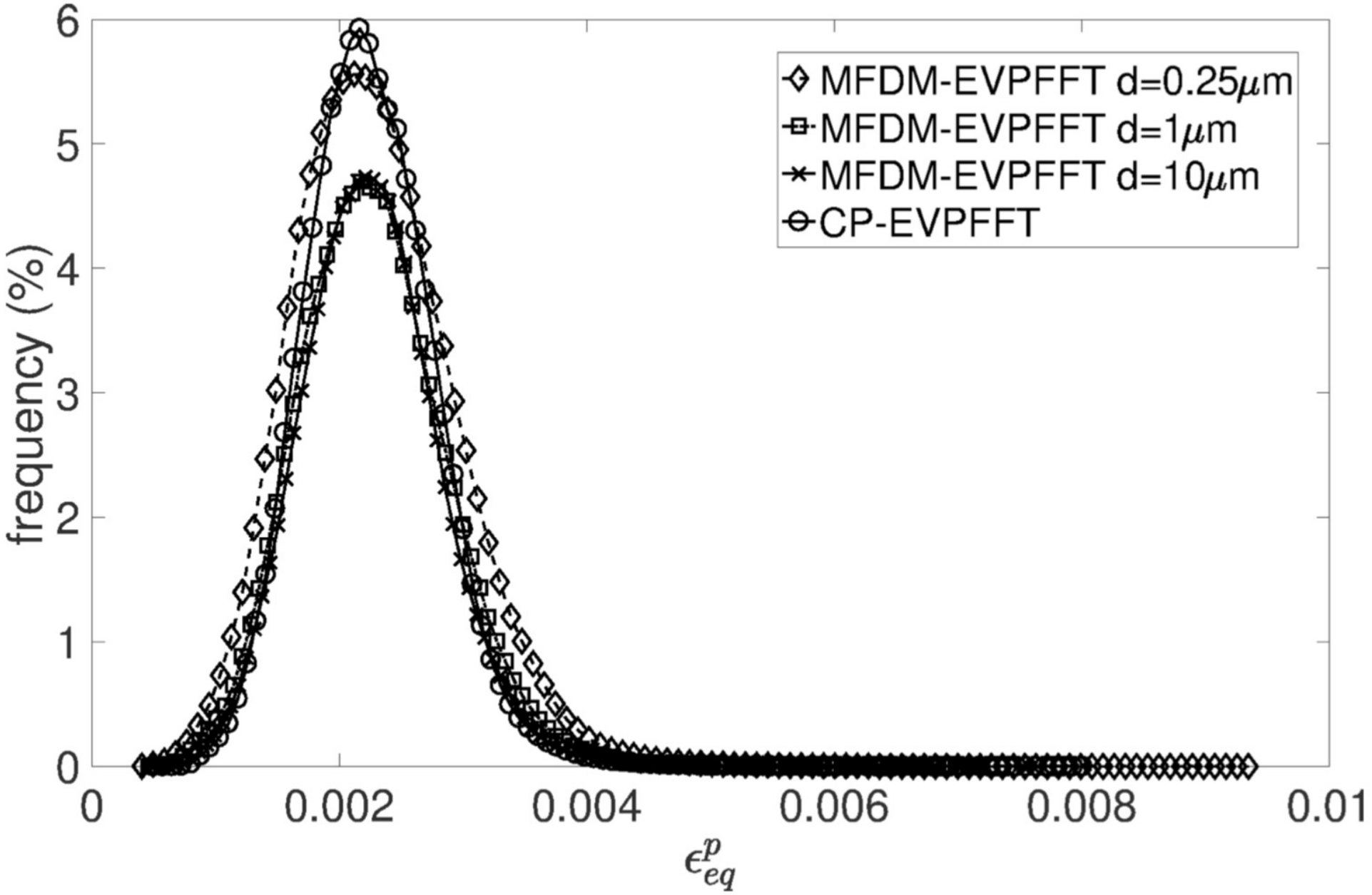
Equivalent Plastic strain

$$p = \varepsilon_p^{eq} = \int_0^t \sqrt{\frac{2}{3}\dot{\boldsymbol{\varepsilon}}^p : \dot{\boldsymbol{\varepsilon}}^p}\, dt$$

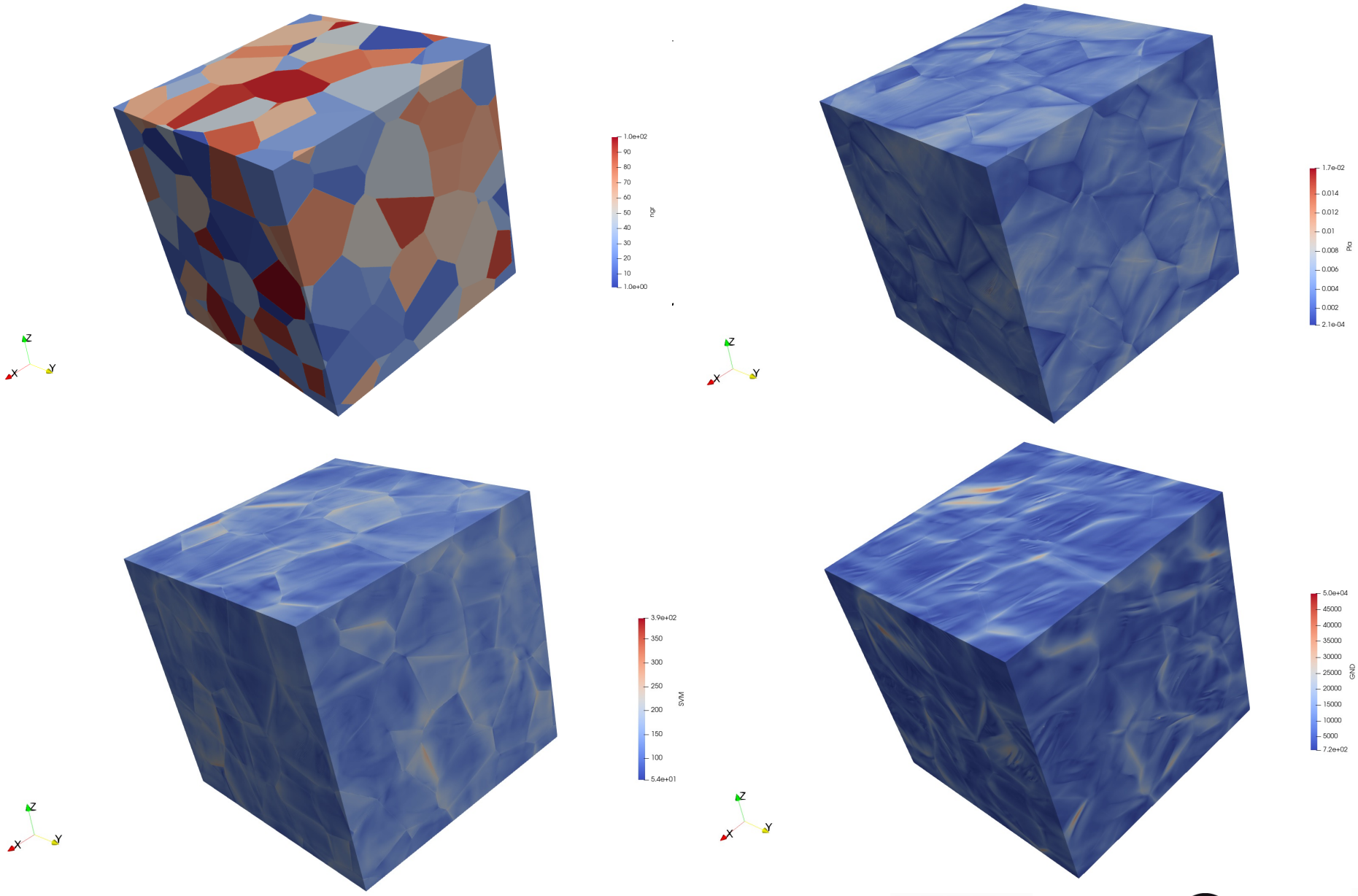


CP-EVP-FFT
(no grain size effect)

Field Histogram



Result with a parallelized version of MFDM-EVPFFT code in LEM3 (MPI): RVE with 512^3 voxels (Explor mesocentre of Univ. Lorraine)



MFDM with defect energy (additional energetic-type hardening)

- **Dissipation:** $D = P_{ext} - \dot{\Phi} = \int_V \mathbf{T}:\dot{\mathbf{U}}dV - \int_V \dot{\phi}dV$ with $\dot{\mathbf{U}} = \dot{\mathbf{U}}^{\mathbf{e}} + \dot{\mathbf{U}}^{\mathbf{p}}$

  with: $\phi = \frac{1}{2}\boldsymbol{\varepsilon}^{\mathbf{e}}:\mathbf{C}:\boldsymbol{\varepsilon}^{\mathbf{e}} + \phi_d(\boldsymbol{\alpha}) = \frac{1}{2}\boldsymbol{\varepsilon}^{\mathbf{e}}:\mathbf{C}:\boldsymbol{\varepsilon}^{\mathbf{e}} + \frac{1}{2}A\,\boldsymbol{\alpha}:\boldsymbol{\alpha}$

  Defect energy density (here quadratic function)

- **Evolution of plastic distortion:** $\dot{\mathbf{U}}^{\mathbf{p}} = \boldsymbol{\alpha}\times\mathbf{v} + \mathbf{L}^{\mathbf{p}}$ with $\mathbf{L}^p = \overline{(\boldsymbol{\alpha}-\overline{\boldsymbol{\alpha}})\times\mathbf{v}} = \overline{\boldsymbol{\alpha}\times\mathbf{v}} - \overline{\boldsymbol{\alpha}}\times\overline{\mathbf{v}}$

- **GND density transport equation:** $\dot{\alpha} = -\mathbf{Curl}\left(\boldsymbol{\alpha}\times\mathbf{v} + \mathbf{L}^{\mathbf{p}}\right)$

  A = constl^2:* non local energetic hardening modulus (l :length scale parameter)

- **Dissipation:** $D = \int_V (\mathbf{T}-\mathbf{B}):\mathbf{L}^{\mathbf{p}}dV + \int_V \mathbf{F}^{\boldsymbol{\alpha}}\cdot\mathbf{v}\,dV$

- **New PK force expression:** $\mathbf{F}^{\boldsymbol{\alpha}} = \mathbf{X}:\mathbf{T}\cdot\boldsymbol{\alpha} + A\mathbf{X}:(\mathbf{curl}\,\boldsymbol{\alpha})^{\mathbf{T}}\cdot\boldsymbol{\alpha} = \mathbf{X}:(\mathbf{T}-\mathbf{B})^{\mathbf{T}}\cdot\boldsymbol{\alpha}$

- **Backstress tensor:** $\mathbf{B} = -A\,\mathbf{curl}\,\boldsymbol{\alpha}$

- **Crystal plasticity due to SSDs:** $\mathbf{L}^{\mathbf{p}} = \sum_{s=1}^{N}\dot{\gamma}^s\mathbf{m}^s\otimes\mathbf{n}^s$ with

$$\dot{\gamma}^s = \dot{\gamma}^0\left(\frac{|\tau^s_{\mathrm{eff}}|}{\hat{\tau}_c}\right)^{1/m}\mathrm{sign}(\tau^s_{\mathrm{eff}})$$

$$\tau^s_{eff} = \tau^s - \tau^s_{kin} \quad \text{and} \quad \tau^s_{kin} = \mathbf{m}^s\otimes\mathbf{n}^s : \mathbf{B}$$

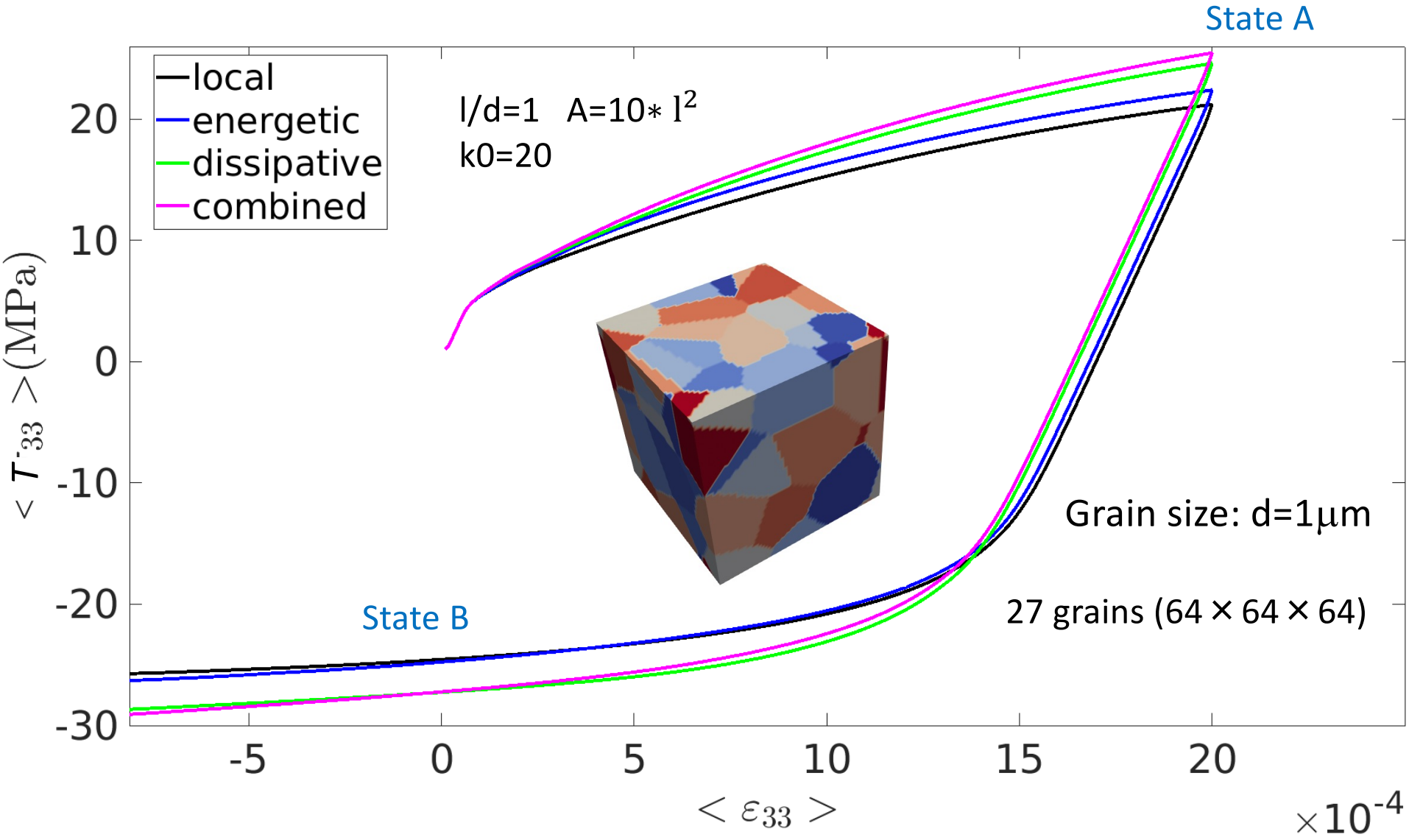
$$\tau^s = \mathbf{m}^s\otimes\mathbf{n}^s : \mathbf{T}$$

- **Backstress evolution for MFDM with defect energy :**

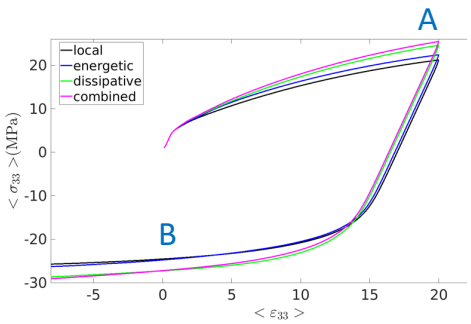
$$\dot{\mathbf{B}} = -A\,\mathbf{curl}\,\dot{\boldsymbol{\alpha}} = A\,\mathbf{curlcurl}\dot{\mathbf{U}}^{\mathbf{p}} = A\left(\boldsymbol{\nabla}\boldsymbol{\nabla}\cdot\dot{\mathbf{U}}^{\mathbf{p}} - \boldsymbol{\nabla}^2\dot{\mathbf{U}}^{\mathbf{p}}\right)$$

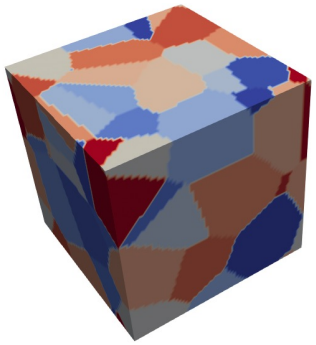
solved with a Fourier-based on centered finite difference scheme for second order derivatives in Fourier space then $\mathbf{B}$ is updated (implicitly) at $t + \Delta t$ (as in Lebensohn and Needleman, JMPS 2016)

Cyclic tensile-compression simulations with PMFDM-EVPFFT



Intragranular fields





dissipative

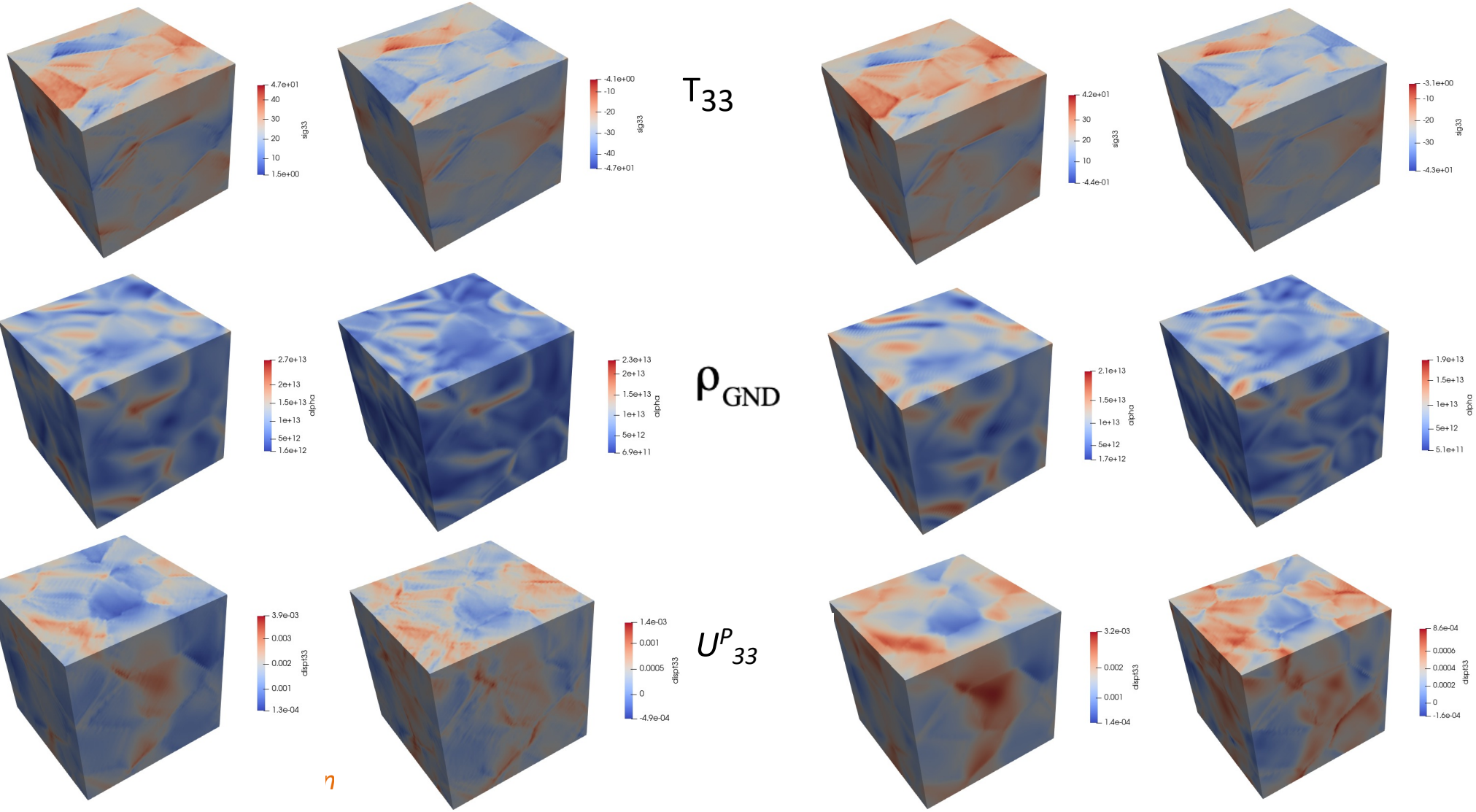
energetic

State A

State B

State A

State B



Summary

- Development of a fast method based on EVPFFT algorithm (Lebensohn et al, 2012) to treat the mechanical fields of mesoscale dislocation mechanics (MFDM) in an EVP formulation → MFDM-EVPFFT
- Plasticity channel/grain size effects (Hall-Petch) were simulated for monotonic loadings and reverse loading (Djaka et al. IJSS 2020, Berbenni et al. JMPS 2020, Genée et al. AMSES 2021)
- Under reverse loading, it is shown that backstress due to dislocation pile up leads to higher kinematical hardening and contributes to Bauschinger effect (dislocation pile up / unpile ups) (Berbenni and Lebensohn CRPhys. 2021)
- Parallelized code MFDM-EVPPFFT developed in LEM3 (under MPI-Fort.)
- Possibility to consider both dissipative/energetic-type hardening in the FFT model (Berbenni et al. EJMSolA N2025)

Present & Perspectives

- Finite strain framework with full MFDM and interfacial conditions, see works by Arora and Acharya 2020-2023 (on Cu-Nb nanolayers)-› FS-MFDM-EVPFFT
- Validations with Discrete Dislocation Dynamics simulations …
- Data bases for developing Machine learning models … (in progress)

Thank you for your attention